

AD-A130 832

STRUCTURE AND PROPERTIES OF INTERCALATED GRAPHITE  
FIBER-POLYMER COMPOSITE..(U) PENNSYLVANIA UNIV  
PHILADELPHIA DEPT OF CHEMICAL ENGINEERING W C FORSMAN

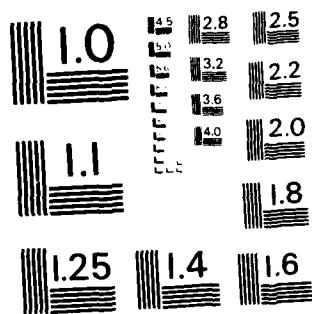
1/1

UNCLASSIFIED

07 JUL 83 ARO-16423.1-MS DAAG29-79-C-0208 F/G 11/4

NL

END  
DATE  
FILMED  
6 83  
DTIC



MICROCOPY RESOLUTION TEST CHART  
NATIONAL BUREAU OF STANDARDS - 1963-A

Unclassified  
SECURITY CLASSIFICATION OF THIS PAGE (When Data Entered)

ARO 16423.1-MS (12)

ADA 13 000 32

DTIC FILE COPY

REPORT DOCUMENTATION PAGE		READ INSTRUCTIONS BEFORE COMPLETING FORM
1 REPORT NUMBER 1	2 GOVT ACCESSION NO. AD-A130832	3 RECIPIENT'S CATALOG NUMBER
TITLE (and Subtitle) STRUCTURE AND PROPERTIES OF INTERCALATED GRAPHITE FIBER-POLYMER COMPOSITES	AUTHOR(s) William C. Forsman	5. TYPE OF REPORT & PERIOD COVERED Final Report
		6 PERFORMING ORG. REPORT NUMBER
PERFORMING ORGANIZATION NAME AND ADDRESS University of Pennsylvania Department of Chemical Engineering Philadelphia, Pennsylvania 19104	CONTROLLING OFFICE NAME AND ADDRESS U. S. Army Research Office Post Office Box 12211 Research Triangle Park, NC 27709	8 CONTRACT OR GRANT NUMBER(s) Grant Number: DAAG29-79-C-0208
		10. PROGRAM ELEMENT, PROJECT, TASK AREA & WORK UNIT NUMBERS
MONITORING AGENCY NAME & ADDRESS (if different from Controlling Office)	12. REPORT DATE July 7, 1983	13 NUMBER OF PAGES 11 pgs. of body, 77 pgs. of Appendixes
		15. SECURITY CLASS. (of this report) Unclassified
16. DISTRIBUTION STATEMENT (of this Report) Approved for public release; distribution unlimited.		15a DECLASSIFICATION/DOWNGRADING SCHEDULE
17. DISTRIBUTION STATEMENT (of the abstract entered in Block 20, if different from Report) Approved for public release; distribution unlimited.		A
18. SUPPLEMENTARY NOTES The view, opinions, and/or findings contained in this report are those of the author(s) and should not be construed as an official Department of the Army position, policy, or decision, unless so designated by other documentation		
19. KEY WORDS (Continue on reverse side if necessary and identify by block number) graphite, graphite fiber, intercalation, acceptor compounds, electrical conductivity composites, interlaminar shear strength, epoxy resins, deintercalation		
20. ABSTRACT (Continue on reverse side if necessary and identify by block number) There is a clear need for high-strength, lightweight composites with improved electrical conductivity. Composites fabricated from intercalated graphite fiber show promise in satisfying that need. This research focused on the chemical aspects of fiber intercalation, stability of intercalated fibers and their relation to the mechanical and electrical properties of their epoxy composites. Early work on this project helped pin down the mechanism of formation of so-called acceptor compounds of graphite as one		

DD FORM 1473 1 JAN 73 EDITION OF 1 NOV 65 IS OBSOLETE

UNCLASSIFIED  
SECURITY CLASSIFICATION OF THIS PAGE (When Data Entered)

83 07 27 00 R 1

Unclassified

SECURITY CLASSIFICATION OF THIS PAGE(When Data Entered)

(20. Abstract - continued)

of oxidation by electron transfer to highly electrophilic species. We then established that, at least in the prototype graphite nitrate, neutral species could be removed under vacuum, and that these labile acid species must be removed before stable composites could be prepared from the intercalated fiber.

In addition, we studied the kinetics of nitric acid intercalation of graphite fiber and powder and highly ordered pyrolytic graphite and offered a proposed mechanism based on crystallite size. Epoxy composites were fabricated from graphite fiber intercalated with nitric acid. At only 3% intercalant (with concomitant increase in fiber conductivity by a factor of 4) the conductivity of composites had increased by a factor of 15, with no degradation of interlaminar shear strength. Intercalating the fiber to the 10% level resulted in a 25% increase in interlaminar shear strength.

Unclassified

SECURITY CLASSIFICATION OF THIS PAGE(When Data Entered)

TABLE OF CONTENTS

	<u>Page</u>
Goal of Research	1
Research Findings	2
Conclusions	5
Publications and Reports	6
Participating Scientific Personnel	7
Appendixes	(numbered separately)
1. "Vapor-Phase Intercalation of Graphite with Nitronium and Nitrosonium Salts"	
2. "Vapor-Phase Intercalation by AlCl <sub>3</sub> -HCl Mixtures"	
3. "Electron Transfer to Protons in Graphite Intercalation"	
4. "Intercalation-Desorption Studies of Graphite Nitrate"	
5. "The System Graphite MnCl <sub>2</sub> -AlCl <sub>3</sub> "	
6. "Acceptor Intercalated Graphite Fibers: Kinetics, Product Stability and Applications to Composites"	
7. "Preliminary Results on the System Graphite-MCl <sub>2</sub> -NO"	
8. "DSC and TGA of Intercalated Graphite Fibers: A Study of Structure and Deintercalation"	
9. "Electrical Conductivity of Composites from Intercalated Graphite Fiber"	
10. "Interlaminar Shear-Strength of Epoxy Composites Fabricated from Intercalated Graphite Fiber"	

GOAL OF RESEARCH

Although graphite fiber/polymer composites have gained wide acceptance, especially in the aerospace industries, they are still deficient in various respects. In particular, if members of this class of composites demonstrated substantially higher electrical conductivity, they would find applications in EMI shielding, as well as structural materials with lightning strick resistance. In addition, the interlaminar shear strength of graphite fiber/polymer composites is inadequate (the fiber surface must be treated to give satisfactory fiber polymer bonding) and their impact resistance leaves much to be desired.

There is reason to believe that composites fabricated from intercalated graphite fiber would go a long way in correcting these deficiencies. Since it is known that intercalation increases the electrical conductivity of graphite fiber, it is clear that their composites would demonstrate electrical conductivity greater than their analogues prepared from pristine fiber. But by how much? In addition, since intercalated fibers have polar surfaces, they should have higher interlaminar shear strength than conventional composites - and possibly better impact resistance as well. But would these possible improvements be realized in practice?

The purpose of this research was thus to study physical and chemical phenomenon associated with fabrication of composites from intercalated graphite fiber, and to examine their implications with regard to properties of the composites.

RESEARCH FINDINGS

Intercalation Chemistry Graphite nitrate fiber serves well as a prototype material for use in assaying the effect of intercalation on composite properties such as electrical conductivity and inter-laminar shear strength. Its limited thermal and environmental stability suggest, however, that it would not have wide applicability in engineering composites. Considerable effort in this project was thus spent in establishing some fundamental chemical principles that could be used in designing reactions that would give more suitable intercalated graphite fibers. In this part of the research, we focused both on pinning down the mechanism of formation of so-called acceptor compounds, and scouting new routes to intercalated graphite fiber. It was in this spirit that we studied intercalation by nitronium and nitrosonium salts, gas-phase  $\text{AlCl}_3\text{-HCl}$  mixtures, liquid adducts of metal chlorides, gas-phase  $\text{MnCl}_2\text{-AlCl}_3$  complexes and gas-phase complexes of NO with metal chlorides.

We are convinced that our contribution to the literature of intercalation chemistry has illuminated the redox nature of graphite intercalation as well as develop several new reactions leading to graphite intercalation compounds. Details are given in the preprints appended to this report.

Although none of these newly discovered reactions have yet been used to prepare intercalated graphite fiber, two of them show great promise. The gas-phase reactions of metal chloride complexes with  $\text{AlCl}_3$  and NO appear to give stable intercalation compounds (which is not surprising since reactions are run between 300 and 500°C).

In addition to the scouting work for new intercalation reactions described above, we prepared two "classical" intercalation compounds from intercalated graphite fiber - the  $\text{AlCl}_3$  and  $\text{FeCl}_3$  compounds. This work was significant, in that it illustrated again that intercalation of graphite fiber effects the same remarkable increase in electrical conductivity as does intercalation of highly oriented pyrolytic graphite. Unfortunately, we judged that the intercalated fibers were too water-sensitive to be of practical use, and did not pursue this line of research any further.

Finally, we documented a non-reductive deintercalation reaction for graphite nitrate, which was observed for intercalated specimens of powder, fiber and HOPG. When kept under dynamic vacuum for a sufficient length of time, virtually all of the intercalant was lost and a product that gave us essentially a graphite x-ray spectrogram was produced. Since no reducing agent was present, we propose the following mechanism:  $\text{NO}_3^-$  diffuses to the surface of the crystalline region, followed by deintercalation through loss of oxides of nitrogen and carbon. We observed the same phenomenon when intercalated HOPG was exposed to reduced pressure but the intercalant loss was far slower. We suggest that the non-reductive deintercalation is slowed down by formation of a protective crust of graphite oxide during the reductive deintercalation effected by interaction with  $\text{H}_2\text{O}$ .

Intercalation Kinetics In a second aspect of this research, we studied the kinetics of intercalation and deintercalation of graphite fiber and powder as well as HOPG. Although reasonable fit to intercalation kinetics could be obtained from a kinetics model containing two arbitrary constants - a nucleation rate for "opening-up" interlaminar

regions and a diffusivity describing transport into the interlaminar regions - we recognize that the approach is essentially empirical. It is not clear, for example, how the nucleation rate is related to the rate of electron transfer from graphite to the nitronium ions. Details are given in the fourth and sixth manuscripts in the appendix.

Composite Properties The final aspect of the research was fabrication of epoxy resin composites from intercalated graphite fibers, and determining their electrical conductivity and interlaminar shear strength. We encountered more practical difficulties than anticipated. They are described in detail in the PhD thesis of T.S. Dziemianowicz and will not be recounted here. Once fabrication "bugs" were worked, however, we were able to establish the following:

- Composites can be fabricated from intercalated graphite fiber provided that corrosive or reactive neutral spacer molecules are first removed from the interlaminar regions. If removed under vacuum, care must be exercised to remove them slowly enough to assure that there is no exfoliation of the intercalated crystalline regions.
- Using graphite nitrate fiber as our prototype intercalated material, we established that:
  1. Short-beam shear strengths of composites can be improved by intercalation of the fiber. Up to 25% improvement over values for conventional composites (prepared from unintercalated fiber were observed.

2. Electrical conductivity of composites can be increased by a factor greater than that for the increase in conduction of the fiber from which they are fabricated. Composites prepared from graphite nitrate with a conductivity only five times greater than that of the pristine fiber gave a composite with a conductivity 14 times greater than its counterpart prepared from the pristine fiber. We propose that this "extra leverage" in improved conductivity is due to (an unexpected) reduced contact resistance with intercalation.

These results are described in detail in manuscripts seven and ten of the appendix.

#### CONCLUSIONS

All things considered, we conclude that the results of this research further support the contention that composites of intercalated graphite may well be an advanced engineering material of the future. There are, however, still serious questions concerning the thermal and environmental stability of intercalated graphite fibers that must be answered before one can predict the future of this class of materials with any certainty.

## PUBLICATIONS AND REPORTS PUBLISHED

- "Vapor-Phase Intercalation of Graphite with Nitronium and Nitrosonium Salts," W.C. Forsman and H.E. Mertwoy, Extended Abstracts, 15th Biennial Conference on Carbon, p. 355, (1981).
- "Vapor-Phase Intercalation by  $AlCl_3$ -HCl Mixtures," K. Leong and W.C. Forsman, Extended Abstracts, 15th Biennial Conference on Carbon, p. 356 (1981).
- "Graphite Intercalation Chemistry: An Interpretive Review," W.C. Forsman, T. Dziemianowicz, K. Leong and D. Carl, Synthetic Metals, 5, 77 (1983).
- "Electron Transfer to Protons in Graphite Intercalation," K. Leong and W.C. Forsman, Synthetic Metals, in press.
- "Intercalation-Desorption Studies of Graphite Nitrate," T. Dziemianowicz, K. Leong and W.C. Forsman, Transactions of the Annual Mtg. Materials Research Society (1982), in press.
- "The System Graphite  $MnCl_2$ - $AlCl_3$ ," T.S. Dziemianowicz, R. Vangelisti, A. Herold and W.C. Forsman, Carbon, in press.
- "Acceptor Intercalated Graphite Fibers: Kinetics, Product Stability and Applications to Composites," W.C. Forsman and T.S. Dziemianowicz, Accepted by Synthetic Metals.
- "Preliminary Results on the System Graphite- $MCl_2$ -NO," K. Leong, A. Tome, T.S. Dziemianowicz, and W.C. Forsman, Accepted by Synthetic Metals.
- "DSC and TGA of Intercalated Graphite Fibers: A Study of Structure and Deintercalation," W.C. Forsman and T.S. Dziemianowicz, Transactions of the 12th Meeting of the North American Thermal Analysis Society, in press.
- "Electrical Conductivity of Composites from Intercalated Graphite Fiber," W.C. Forsman, F.L. Vogel, and C. Zeller, submitted to Synthetic Metals.
- "Interlaminar Shear-Strength of Epoxy Composites Fabricated from Intercalated Graphite Fiber," W.C. Forsman and T.S. Dziemianowicz, submitted to Carbon.
- "Reductive and Nonreductive Deintercalation of Graphite 'Acceptor' Compounds," W.C. Forsman, T.S. Dziemianowicz and W. Beckmann, in preparation.
- "Intercalation of Graphite Fiber: A Short Review," W.C. Forsman and T.S. Dziemianowicz, in preparation.
- Other manuscripts in preparation from the PhD theses of T.S. Dziemianowicz and K. Leong.

## PARTICIPATING SCIENTIFIC PERSONNEL

W.C. Forsman	Principal Investigator
T.S. Dziemianowicz	Graduate Student PhD granted, June 1983
K. Leong	Graduate Student PhD to be granted, December 1983
H.E. Mertwoy	Research Specialist
B. Folgherait	Graduate Student

## APPENDIXES

The following are copies of preprints and short publications generated by this grant in the order they appear in "Publications and Reports Published." In the interest of space, the long paper (24 pages) "Graphite Intercalation Chemistry: An Interpretive Review" is not included since it has been in print for several months.

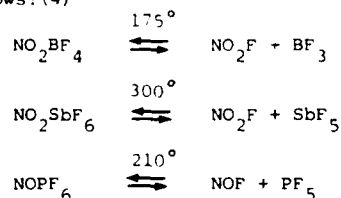
Vapor-Phase Intercalation of Graphite with Nitronium and Nitrosonium Salts

[Appendix 1]

W. C. Forsman and H. E. Mertwoy  
Department of Chemical Engineering  
University of Pennsylvania  
Philadelphia, Pennsylvania 19104

Recent studies have shown that the action of solutions of both nitronium  $\text{NO}_2^+$  (1,2) and nitrosonium  $\text{NO}^+$  (3) salts of  $\text{BF}_4^-$ ,  $\text{PF}_6^-$  and  $\text{SbF}_6^-$  on HOPG produce intercalated compounds which are much more highly conducting than the original graphite. Experimental evidence (1,2) indicated that the electrophilic  $\text{NO}_2^+$  and  $\text{NO}^+$  ions were approximately equally effective in capturing electrons from the graphite lattice, resulting in anion insertion. The experimental results (1,3) also indicated that neutral nitronium or nitrosonium molecules and solvent molecules may have intercalated along with the anions.

We have now established that HOPG can be intercalated to form highly conducting materials by reaction with the vapors of the decomposition products of nitronium tetrafluoroborate ( $\text{NO}_2\text{BF}_4$ ), nitronium hexafluoroantimonate ( $\text{NO}_2\text{SbF}_6$ ) and nitrosonium hexafluorophosphate ( $\text{NOPF}_6$ ). These salts when heated above the indicated temperatures dissociate reversibly as follows: (4)



Experimental

Nitronium tetrafluoroborate was prepared from fuming nitric acid, hydrofluoric acid and boron trifluoride in a nitromethane solution using the method described by Kuhn and Olah (4). Some of the experiments were carried out using  $\text{NO}_2\text{BF}_4$  purchased from Ventron Chemical Co. Nitronium hexafluoroantimonate and nitrosonium hexafluorophosphate were purchased from Ventron Chemical Company. Since nitronium and nitrosonium salts are very hygroscopic and subject to hydrolysis they were heated in vacuo at  $100^\circ\text{C}$  for several hours before using to remove hydrolysis products ( $\text{HNO}_3$ ,  $\text{HF}$ , and  $\text{BF}_3$ , or  $\text{SbF}_5$ , or  $\text{BF}_5$ ). Transfer of all materials was carried out in a dry box.

Intercalation experiments were performed with highly oriented pyrolytic graphite (HOPG) crystals supplied by Dr. Arthur Moore of the Union Carbide Corporation. They were dried at  $100^\circ\text{C}$  in vacuo before each intercalation experiment. In experiments with dry nitronium and nitrosonium salts, an HOPG crystal was heated in the same dried and evacuated tube (or a 250 ml flask) with the salt. No attempt was made to maintain the HOPG at a higher temperature than the salt. Other experiments were

done with undried salts, some of which appeared caked and obviously contained hydrolysis products. Except for cases where rapid intercalation resulted in exfoliation of the intercalation compound, volume resistivities of all complexes were determined both before and after reaction by the technique of Zeller, et. al. (5).

Results

Intercalations run at 210 and  $300^\circ\text{C}$  with dry  $\text{NOPF}_6$  and  $\text{NO}_2\text{SbF}_6$  respectively went so rapidly that every attempt resulted in an exfoliated compound. Most reactions with dry  $\text{NO}_2\text{BF}_4$  at  $180^\circ\text{C}$ , went in a well controlled manner, but even in this case several HOPG specimens exfoliated before the reaction was completed. Reactions of HOPG with dry  $\text{NO}_2\text{BF}_4$  effected increases in weight of 25-30%, increases in thickness of 30-35% and decreased the volume resistivity by a factor of about 0.1

Surprisingly, we found that HOPG exposed to the vapor in equilibrium with undried  $\text{NO}_2\text{BF}_4$  and  $\text{NOPF}_6$  intercalated at low temperature. Indeed, the volume resistivity of HOPG decreased by a factor of about 0.5 within a few minutes after exposure to the vapor in equilibrium with undried  $\text{NO}_2\text{BF}_4$  at room temperature. Since  $\text{HNO}_3$  is one of the hydrolysis products, what we may have observed was nitric acid intercalation, but the phenomenon is being explored further.

Conclusions

We conclude that  $\text{NO}_2\text{F}$  adsorbed at the vapor-graphite interface reacts with adsorbed  $\text{MF}_5$  to form  $\text{NO}_2^+$  and  $\text{MF}_6^-$ . The adsorbed  $\text{NO}_2^+$  captures electrons from the graphite effecting intercalation of  $\text{MF}_6^-$  and (possibly) neutral molecules. The same mechanism would apply to vapor mixtures of  $\text{NOF}$  and  $\text{MF}_5$ .

Acknowledgement

This work was funded by the Army Research Office through Grant Number DAAG29-79-C-0208.

References

1. W.C. Forsman and H.E. Mertwoy, *Synthetic Metals*, 2, 171 (1980).
2. D. Billaud, A. Pron, and F.L. Vogel, *Synthetic Metals*, 2, 177 (1980).
3. W.C. Forsman and H.E. Mertwoy, *Carbon*, in press.
4. S.J. Kuhn and G.A. Olah, *J.A.C.S.*, 83, 4563 (1961).
5. C. Zeller, G.M.T. Foley, E.R. Falardeau, and F.L. Vogel, *Materials Sci. and Eng.*, 31, 255 (1977).
6. W. Rudorff in "Advances in Inorganic Chemistry and Radio Chemistry", 1, (eds. H.J. Emeleus and A.G. Sharpe, Acad. Press, 1959, p. 231.

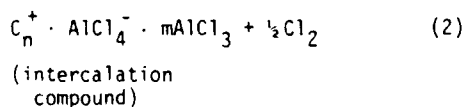
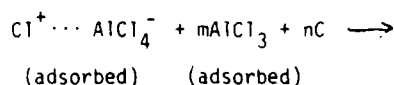
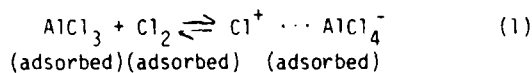
## Vapor-Phase Intercalation by $\text{AlCl}_3$ -HCl Mixtures

[Appendix 2]

Kam Leong and W. C. Forsman  
 Department of Chemical Engineering  
 University of Pennsylvania  
 Philadelphia, Pennsylvania 19104

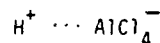
### Introduction

One of us (1) suggested that vapor-phase intercalation by  $\text{AlCl}_3$  in the presence of  $\text{Cl}_2$  proceeds by the following mechanism:



The structure  $\text{Cl}^+ \cdots \text{AlCl}_4^-$  could be either a pair of ions or a highly polar chlorine-aluminum chloride complex. In either case, the driving force for intercalation is electron transfer from graphite to the highly electrophilic, positively charged chlorine. Chlorine radicals formed by the electron transfer would couple and be released as chlorine gas, and  $\text{AlCl}_4^-$  ions along with  $\text{AlCl}_3$  molecules would intercalate the lattice.

This mechanism suggests that HCl could serve as the coreagent for intercalation by  $\text{AlCl}_3$ . In this case the pair of ions or complex would be



The intercalating species would probably be the same, but because of the high reactivity of the hydrogen atoms formed by the electron-transfer reaction, various side products could be formed.

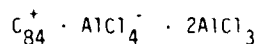
This paper reports that graphite is indeed intercalated by a gas-phase mixture of  $\text{AlCl}_3$  and HCl.

### Experimental

The conventional two zone technique was used, with HOPG crystals as host materials. Commercially available  $\text{AlCl}_3$  was purified by vacuum sublimation in the presence of aluminum metal at least five times. An atmosphere of 500 torr of HCl was introduced into the reaction tube before it was sealed off. The graphite end was heated at 200°C, and the  $\text{AlCl}_3$  end 180°C. X-ray and conductivity measurements were taken in situ.

### Results

The sample demonstrated a weight gain of 39% and its electrical conductivity increased by a factor of 11.0. This would correspond approximately to a fourth stage compound with an empirical formula of



Noteworthy is the close similarity between this compound's X-ray pattern and the fourth stage compound prepared with chlorine and  $\text{AlCl}_3$ . The intensities and positions of the diffraction peaks match well with one another. The identity layer spacing of  $19.64 \pm 0.05\text{\AA}$  also compares well to the value of  $19.67 \pm 0.02\text{\AA}$  found in the conventional compound (2). This suggests that identical intercalants and structure are obtained by both routes.

### Acknowledgements

This work was supported by the Army Research Office through Grant Numbers DAAG29-79-C-0208 and DAAG29-78-0037. The HOPG was donated by the Union Carbide Corporation through the good offices of Dr. Arthur Moore.

### References

1. W. C. Forsman, Extended Abstracts, Thirteenth Biennial Conference on Carbon, p. 153, (1977)
2. G. M. Gualberto, C. Underhill, S. Y. Leng, and G. Dresselhaus, Physical Review B., 21, 962 (1980)

## SYNTHETIC METALS

HM

AUTHOR	<input checked="" type="checkbox"/> EDITOR	MASTERCOPY	3 pages	SYM 187
QUERIES	<input type="checkbox"/> CORRECTION	Vol. No. pp.		

Only typographical correction will be accepted at this stage.

*Synthetic Metals,*

[Appendix 3]

## Short Communication

## Electron Transfer to Protons in Graphite Intercalation

K. LEONG and W. C. FORSMAN

*Department of Chemical Engineering, University of Pennsylvania, Philadelphia, PA 19104 (U.S.A.)*

(Received November 24, 1982)

Graphite is intercalated by the vapor-phase mixture of HCl and AlCl<sub>3</sub>. Reactions at 200 °C give a stage-4 compound; a weight increase of 39% is observed and the electrical conductivity increases by a factor of eleven. Hydrogen and methane are produced during intercalations along with trace amounts of higher hydrocarbons. The results clearly indicate that electron transfer between the graphite lattice and the proton in the complex H<sup>+</sup> ... AlCl<sub>4</sub><sup>-</sup> is the driving force for the reaction. The hydrogen atoms generated by the electron transfer either couple to form hydrogen gas or attack the graphite lattice to form hydrocarbons.

One of us [1] has offered evidence that the driving force for most intercalation reactions that give so-called "acceptor compounds" is electron transfer from the graphite lattice to a highly electrophilic species. A second product of the electron transfer is always formed which can be a stable compound or a highly reactive species that undergoes further reaction. In the case of electron transfer to nitronium and nitrosonium ions (NO<sub>2</sub><sup>+</sup> and NO<sup>+</sup>), the second product is an oxide of nitrogen which is released as a gas or, in the case of solution-phase intercalation, may dissolve in the solvent [1-5].

Intercalation of graphite by metal chlorides offers an interesting example of that class of intercalations in which electron transfer to the electrophile gives a highly reactive free radical species. Until recently, however, the evidence for this mechanism has been circumstantial. The argument has proceeded as follows.

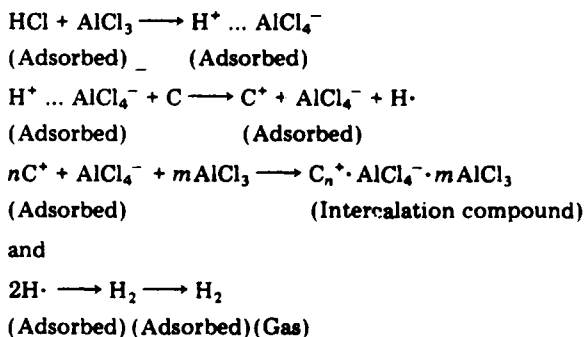
Intercalation of graphite by metal chlorides is dramatically affected by the presence of chlorine. In the case of non-oxidizing metal chlorides such as AlCl<sub>3</sub>, ZnCl<sub>2</sub> and MnCl<sub>2</sub>, no intercalation occurs unless chlorine is added to the reaction system. Metal chlorides that do not require the presence of chlorine for intercalation of graphite, as in the case of FeCl<sub>3</sub> and CuCl<sub>2</sub>, are known to provide Cl<sub>2</sub> to the reaction through decomposition to a lower valency chloride. In every case, it is without dispute that rate of intercalation is increased by the presence of chlorine [6]. The role played by chlorine has, however, been the subject of much debate; does it play the role of catalyst or reactant? The view held by this laboratory [1] is that the chlorine, along with AlCl<sub>3</sub>, serves as the reactant.

The fact that neither chlorine [7] nor aluminum chloride alone intercalate graphite strongly suggests the participation of a Friedel-Crafts complex. One can then argue [1] that intercalation is effected by the species  $\text{Cl}^+ \dots \text{AlCl}_4^-$ , which could either be a pair of ions or a highly polar complex adsorbed at the graphite surface. The driving force is electron transfer from graphite to the highly electrophilic, chlorine cation. The chlorine atom formed by the electron transfer would couple to form chlorine gas, a reaction product which would not serve as evidence for the mechanism. According to the postulated mechanism, HCl would also be a candidate as a co-reagent in intercalation by  $\text{AlCl}_3$ . The attacking species in this case, however, would be  $\text{H}^+ \dots \text{AlCl}_4^-$ , a reagent that has been alluded to in many of the Friedel-Crafts reactions, for instance, protolysis of alkanes to alkylcarbonium ions [8].

We recently demonstrated that a gas phase mixture of  $\text{AlCl}_3$  and HCl does, indeed, effect the intercalation of graphite [9]. Highly oriented pyrolytic graphite (HOPG) was intercalated using the conventional two zone technique. The HOPG demonstrated a weight gain of 39% and an increase in electrical conductivity of a factor of 11. An X-ray diffractogram indicated that the product was a stage-4 intercalation compound with spacings almost identical with those for compounds prepared from the  $\text{Cl}_2$ - $\text{AlCl}_3$  mixture.

We have now repeated the experiments using graphite powder as host materials. The powder was extensively outgassed under high vacuum. As before, purified  $\text{AlCl}_3$  was sublimed into the reaction tube which had a break-sealed end. An atmosphere of 600 Torr of HCl was employed. In this series of experiments, however, the gaseous reaction products were analyzed using a mass spectrometer. As in our previous experiments, X-ray diffractometer measurements positively indicated that the product was an intercalation compound of approximately a fourth stage.

The mass spectrometer analysis indicated that the major side-product of the reaction was hydrogen, with the formation of about one-tenth that molar quantity of methane and traces of higher molecular weight hydrocarbons. The amount of hydrogen and methane formed was consistent with the mechanism:



$H \cdot + C \longrightarrow$  Hydrocarbons

The hydrogen that is formed could only come from electron capture by the reactive hydronium end of the  $HCl-AlCl_3$  complex.

It should be noted, however, that the  $H^+AlCl_4^-$  complex itself has not been isolated but is believed to exist in the presence of a proton acceptor [10]. Graphite certainly qualifies by its excellent electron donating ability. The electrophile ' $Cl^{++}$ ' is, however, more reactive, and its complexation with graphite should be favoured by supplementary d-pi interaction. Indeed, a much lower threshold vapor pressure is observed for  $Cl_2$  than for  $HCl$ . Inter-calation proceeds rapidly with catalytic amounts of chlorine, whereas several hundred torr of hydrogen chloride are required.

#### Acknowledgement

This work was supported, in part, by the Army Research Office through Grant Number DAAG29-79-C-0208.

#### References

- 1 W. C. Forsman, *Ext. Abstr., 13th Biennial Conf. on Carbon*, (1977), p. 153.
- 2 W. C. Forsman, D. E. Carl and F. L. Vogel, *Carbon*, 16 (1978) 269.
- 3 W. C. Forsman and H. E. Mertwoy, *Synth. Met.*, 2 (1980) 171.
- 4 W. C. Forsman and H. E. Mertwoy, *Carbon*, in press.
- 5 W. C. Forsman and H. E. Mertwoy, *15th Biennial Conf. on Carbon*, p. 355 (1981).
- 6 A. R. Feichtinger, A. Baiker and W. Richarz, *Ext. Abstr., 15th Biennial Conference on Carbon*, (1981), p. 375.
- 7 Graphite-chlorine is formed only in liquefied chlorine below room temperatures. G. Furdin, M. Lelanrain, E. McRae, J. F. Marceche and A. Héroid, *Carbon*, 17 (1979) 329.
- 8 H. Pines and R. C. Wackher, *J. Am. Chem. Soc.*, 68 (1946) 595.
- 9 K. Leong and W. C. Forsman, *15th Biennial Conf. on Carbon*, (1981), p. 356.
- 10 H. C. Brown and H. W. Pearsall, *J. Am. Chem. Soc.*, 73 (1951) 4681.

## INTERCALATION-DESORPTION STUDIES OF GRAPHITE NITRATE

T. DZIEMIANOWICZ, K. LEONG, AND W.C. FORSMAN  
Department of Chemical Engineering, University of Pennsylvania  
Philadelphia, PA 19104

## ABSTRACT

A new model for intercalation kinetics is presented which takes into account both nucleation of the interlamellar spaces and intercalant layer growth. For nitric acid intercalation, the nucleation constant,  $\beta$ , ranges from  $1.25 \times 10^{-3}$  to  $10^{-4} \text{ sec}^{-1}$  depending on graphite type (HOPG > powder > fibers); the corresponding range of effective diffusivities,  $D$ , is  $2.5 \times 10^{-5}$  to  $10^{-10} \text{ cm}^2/\text{sec}$ . It is emphasized that effective diffusivities obtained from sorption kinetics are reaction enhanced.

Stepwise isothermal desorption experiments show that the diffusivities of  $\text{HNO}_3$  neutrals are lower than the effective diffusivities on sorption. At desorptive equilibrium, intercalant retention is in the order HOPG > powder > fibers. In HOPG, resistance is constant over the desorptive transition stage II  $\rightarrow$  III  $\rightarrow$  IV; during the stage IV  $\rightarrow$  V  $\rightarrow$  VI regime (dynamic vacuum), resistance doubles. A similar resistance gain is noted on desorption of neutrals from nitrated graphite fibers.

## INTRODUCTION

Graphite intercalation compounds (GIC's) have been shown to possess a number of interesting physical and chemical properties, not the least of which is the potential for extraordinary a-axis (i.e., along the carbon planes) electrical conductivity. It remains to be seen, however, how effectively such "laboratory curiosities" may be parlayed into useful engineering materials. In this regard, two central issues are (1) how, and in what form can intercalation compounds be combined with other materials to yield a useful product, and (2) how can GIC's be stabilized to mitigate the effects of hostile environments. In a sense it is the latter question which is the more urgent, since it is well known that GIC properties may be radically altered once removed from an equilibrium environment.

Earlier work in this laboratory has focused on the chemistry and properties of graphite nitrate compounds. Though lacking in at least one important practical consideration -- thermal stability -- graphite nitrate is in many other respects a suitable model system for studies of potential applications. The synthesis [1], chemistry [2], structure and properties [3] have been scrutinized as closely as in most other acceptor-type compounds. Relatively high conductivities ( $4 \times 10^5 \text{ } \Omega\text{-cm}^{-1}$  for stage 2) have been reported [4]; furthermore, preliminary studies show that the electrical properties are relatively insensitive to intercalant concentration at least over the range stage 2-4 [5]. Finally, the reaction is an economical one, both in terms of time and energy requirements -- it proceeds rapidly at room temperature -- and in that the raw material cost of the intercalant (or its precursors) is small

investigate the nature of isothermal intercalation-desorption behavior in the system graphite-HNO<sub>3</sub> with an eye toward mechanistic insights and the effects of desorption on the structure, properties and stability of nitrate GIC's.

### EXPERIMENTAL

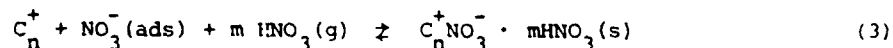
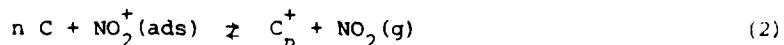
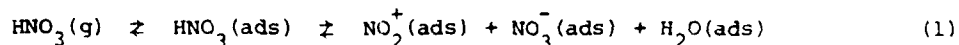
Four different grades of graphite were studied. HOPG (Union Carbide) was in form of thin plaques 0.5 cm. on a side. Natural graphite (Superior Graphite Co.) was a fine powder of particle size 44u. Graphite fibers were either PAN-based GY-70 (Celanese) or pitch-based VS-0054 (Union Carbide); the former were obtained without sizing, and the latter were heated at 350°C overnight to remove a light surface finish. Immediately prior to each intercalation, fresh HNO<sub>3</sub> was prepared by dripping 96% H<sub>2</sub>SO<sub>4</sub> onto KNO<sub>3</sub> and collecting the room temperature distillate over liquid N<sub>2</sub>. The nitric acid prepared in this fashion has a vapor pressure of 80-90% of that reported for pure HNO<sub>3</sub> [6]. By interpolation, this corresponds to 97-98% HNO<sub>3</sub>. The apparatus for measuring weight uptake has been described previously [2] (spring balance, cathetometer, combined precision ± 0.05 mg.); in situ conductivity measurements on HOPG were by a contactless technique [7], and a four-point technique was used for mounted single fibers [8]. Stage determination was accomplished by diffractometer (MoKα) radiation (HOPG), or by Debye-Scherrer technique (CuKα) for powders and fibers (beam perpendicular to fiber axis).

Room temperature desorption was accomplished simply by varying the temperature of the HNO<sub>3</sub> reservoir. The range of nitric acid pressures employed was thus 25 torr (intercalation at T<sub>HNO<sub>3</sub></sub> = 15°C, 10 torr (ice bath, 0°), 1.8 torr (CCl<sub>4</sub> slush; -23°), -0 torr (liquid N<sub>2</sub>; -196°), and dynamic vacuum. Depending on the form of the graphite, weight uptake, conductivity and x-ray measurements (the latter at widely spaced intervals) were performed during the course of desorption. After desorption, long term stability was monitored under ambient conditions (moist air), or in dry air (over anhydrous CaSO<sub>4</sub>).

### RESULTS AND DISCUSSION

#### Intercalation kinetics

The chemistry of nitric acid intercalation has been investigated by Forsman, et al. [2]. The proposed reaction mechanism involves three steps -- adsorption and dissociation, oxidation and insertion -- which are described by the equations:



It is presumed that step (2) is irreversible. A number of investigators have modelled the intercalation of nitric acid into HOPG [9] and graphite fibers [10] using a simple Fickian diffusion approach. Treatments of this type (for other intercalant systems as well) have met with limited success. The kinetic data cannot be fit with a single apparent diffusivity over the entire concentration range; a better correlation may be obtained if the diffusivity is allowed to vary with intercalant content [11]. More importantly, it can be shown that the boundary condition used in this approach,

$$c_0(R) = c_{\infty}, \quad t > 0 \quad (4)$$

(i.e., that the edges of all the interlaminar spaces are nucleated instantly to their equilibrium content,  $c_{\infty}$ ) demands that the weight uptake curve be always concave to the time axis\*. Yet, experimental data -- when taken at sufficiently short times -- give sigmoidal curves. The initial convex portion is often referred to as the induction period. Bardhan and Chung [12] have used surface profilometry to show that rates of both nucleation and intercalant layer growth may influence global kinetics. This suggests a two parameter model for treatment of weight uptake as well. Transport within a layer will be assumed Fickian with an apparent diffusivity  $D$ , and nucleation of layers will be taken as first order in the number of vacant interlaminar spaces. The boundary condition thus becomes

$$c_o(R) = c_{\infty}(1 - e^{-\beta t}) \quad (5)$$

(Bardhan and Chung assumed zeroth order nucleation,

$$c_o(R)/c_{\infty} = \beta t, \quad 0 < t < 1/\beta; \quad c_o(R)/c_{\infty} = 1, \quad t \geq 1/\beta \quad (6)$$

We have chosen condition (5) instead both for its realistic physical interpretation -- i.e., saturation-type behavior -- and for greater ease in solution of the relevant differential equation). The solution for unsteady state radial diffusion in a cylinder or disk of radius  $R$ , with boundary condition (5) is given by Crank [13]. If we define a characteristic diffusion time,

$$\tau_D = R^2/D, \quad (7)$$

and a characteristic nucleation time,

$$\tau_N = 1/\beta, \quad (8)$$

and their ratio,  $\Theta = \tau_D/\tau_N$ , the solution may be written in terms of these parameters,

$$\frac{M(t)}{M_{\infty}} = 1 - \frac{2 J_1(\Theta^{1/2})}{\Theta^{1/2} J_0(\Theta^{1/2})} e^{-t/\tau_N} + 4 \sum_{n=1}^{\infty} \frac{\exp(-c_n^2 \frac{t}{\tau_D})}{c_n^2 (\frac{c_n}{\Theta} - 1)} \quad (9)$$

Here  $J_0$  and  $J_1$  are the Bessel functions of the first kind of order zero and one respectively, and the  $c_n$  are roots of  $J_0(c_n) = 0$ . Plots of (9) are initially convex to the time axis before turning concave at longer reaction times. Furthermore, it is easily verified that when  $\tau_D \gg \tau_N$ , the first exponential in (9) decays rapidly, and the diffusion controlled solution is obtained, whereas if  $\tau_N \gg \tau_D$ , the series of exponentials vanishes quickly, and one obtains the nucleation controlled solution which was proposed by Metz and Siemsgluss [14].

Figure 1 shows that the agreement between the nucleation/diffusion model and experimental data for  $\text{HNO}_3$  intercalation is quite good, both in terms of the shape of the curve, and in spanning the entire concentration range. The only notable deviation is the "shoulder" in the HOPG data at  $\Delta m/m_{\infty} = 0.75$ . This is probably due to a stage III-II structural transition, which is beyond the scope of the model. It must be emphasized that  $D$  in equation (9) is an *effective* diffusivity -- that is, in reality, it lumps together a number of physico-chemical phenomena, only one of which is diffusion into the lattice (among the other processes may be chemisorption of  $\text{NO}_3^-$  ions subsequent to lattice oxidation, as in equations (2,3), and mechanical resistance of the

\*A proof attributed to Prager is given in reference [13], p. 180.

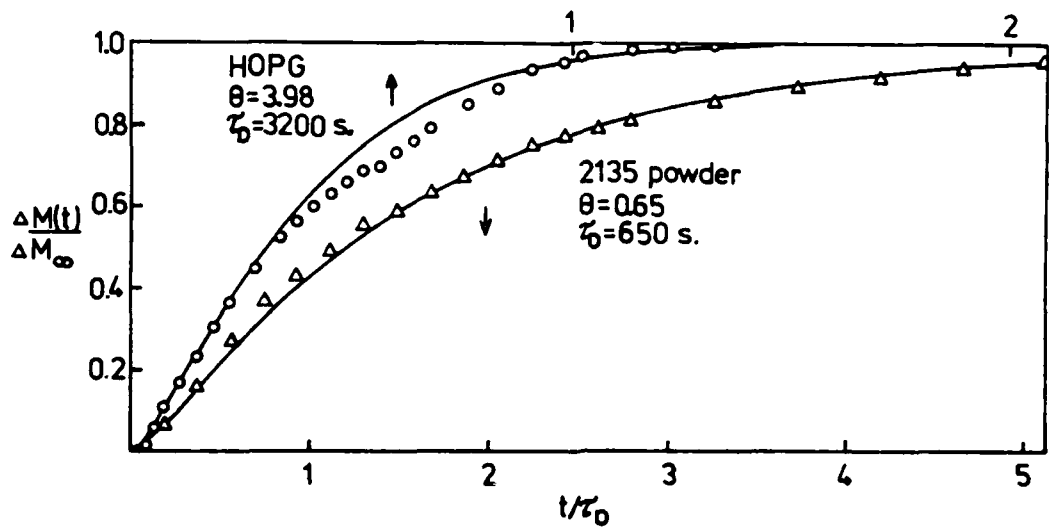
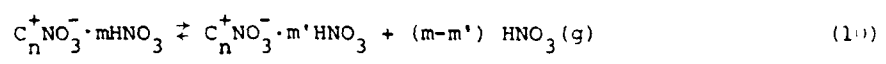


Figure 1. Nucleation/diffusion model as applied to nitric acid intercalation (equation 9 (—); experimental data (o,Δ)).  $T_G = 25^\circ\text{C}$ ,  $P_{\text{HNO}_3} = 25$  torr.

lattice to intercalant penetration). The summary of model parameters obtained by curve fitting to experimental data (Table 1) shows that nitric acid intercalation into HOPG is closest to a diffusion controlled reaction ( $\theta > 1$ ), whereas in powder and fibers, the initial reaction events play a greater role in the kinetics ( $\theta < 1$ ).

Desorption results

It has been postulated that -- at least in the initial stages -- desorption of a saturated intercalation compound proceeds simply by efflux of the neutrals according to (e.g., in the case of nitric acid compounds)



This suggests that the kinetics of this process may be treated and interpreted somewhat more simply than on weight uptake (intercalation). If only small amounts of neutrals are desorbed such that there are no structural changes, and we postulate that transport out of the graphite occurs by Fickian diffusion with an effective diffusivity  $D'$ , the weight loss as a function of time (again assuming a disk-like or cylindrical geometry) is given by [13]:

$$\frac{\Delta M(t)}{\Delta M_\infty} = 1 - 4 \sum_{n=1}^{\infty} \frac{\exp(-c_n^2 t / \tau_D)}{c_n^2} \quad (11)$$

where  $\tau_D = R^2/D'$  and the  $c_n$  are as described previously. As long as the driving force for diffusion is small (i.e., change in  $P_{\text{HNO}_3}$  from 25 torr to 10 torr), the kinetic data fit a simple diffusion model fairly well; when more drastic measures are taken to promote efflux of the neutrals (there is little desorption from fibers, for example, except under dynamic vacuum), the agreement is not nearly as good. Desorption parameters for various graphites are listed in Table 1

TABLE 1

Intercalation and desorption parameters for nitric acid intercalation of various graphites ( $T_G = 25^\circ\text{C}$ ;  $p_{\text{HNO}_3} = 25$  torr).

Graphite type	Weight uptake $\Delta M_\infty/M_0$	$\beta$ ( $\text{sec}^{-1}$ )	$D$ ( $\text{cm}^2/\text{s}$ )	$\theta$ ( $=\tau_D/\tau_N$ )	$D'$ ( $\text{cm}^2/\text{s}$ )	Content after desorp. $\Delta M/M_0$
HOPG	0.502	$1.25 \times 10^{-3}$	$2.5 \times 10^{-5}$	4.0	$7.5 \times 10^{-6}$ *	0.15
2135	0.492	$1 \times 10^{-3}$	$7.5 \times 10^{-9}$	0.6	$1.5 \times 10^{-9}$ *	0.028
P-100 (VS-0054)	0.467	$5 \times 10^{-4}$	$5 \times 10^{-10}$	0.3	$\sim 1 \times 10^{-11}$ +	0.099
GY-70	0.353	$1.35 \times 10^{-4}$	$1 \times 10^{-10}$	0.2	$\sim 1 \times 10^{-11}$ +	0.10

\*Desorption at  $p_{\text{HNO}_3} = 10$  torr

+Desorption under  $3$  dynamic vacuum

Figure 2 shows the kinetics of weight loss during step-wise desorption in HOPG and 2135 powder. It is noteworthy that the HOPG retains much more intercalant at desorptive equilibrium than does the powder. This may reflect differences in morphology; the HOPG has smaller crystallites and hence more grain boundary per unit volume of material. If the residual intercalant is preferentially located near high energy sites such as these, the HOPG would be expected to retain more. It is possible that a similar effect is manifest in the parameters  $D$  and  $D'$ . Both are greater in HOPG, suggesting that resistance to penetration of the intercalant is weaker along the crystallite boundaries than it is for transport through crystalline regions. It should also be noted that  $D'$  is always substantially less than  $D$ , supporting the concept that  $D$  is a reaction enhanced diffusivity.

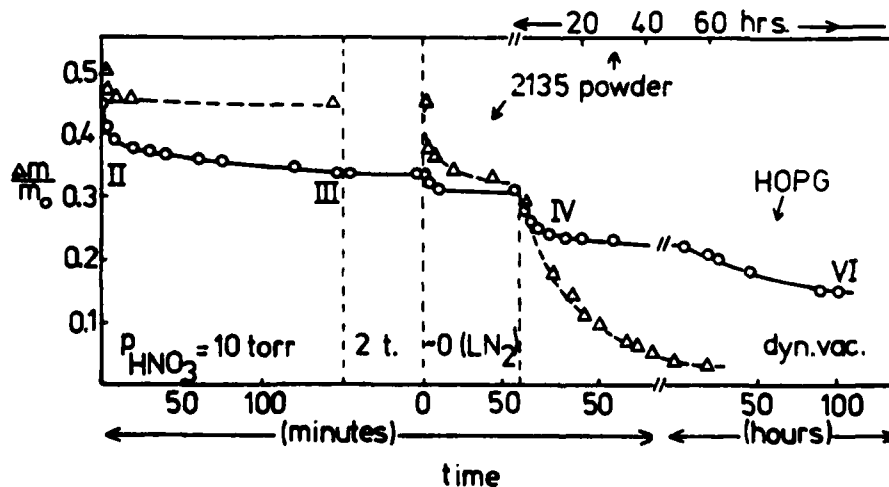


Figure 2. Stepwise isothermal desorption of stage II graphite nitrates at  $25^\circ\text{C}$  (HOPG -  $\circ$ ; 2135 powder -  $\Delta$ ).

As reported previously [5], no changes in electrical resistance were observed on desorption from stage II to stage IV in HOPG. Beyond stage IV, however, resistance increases, roughly doubling by the time equilibrium is attained at stage VI. Whether this is due to a change in the ionic content (unlikely according to equation 2), diminished mobility within the intercalant layers as more neutrals are removed, or structural changes such as diminished domain size, remains to be seen. It would also be interesting to examine electrical changes in the powder on desorption, since the implication is that charge transfer must be much less in this compound as it gives up its intercalant so readily. Similar increases in resistance are observed on desorption of graphite fibers (Figure 3).

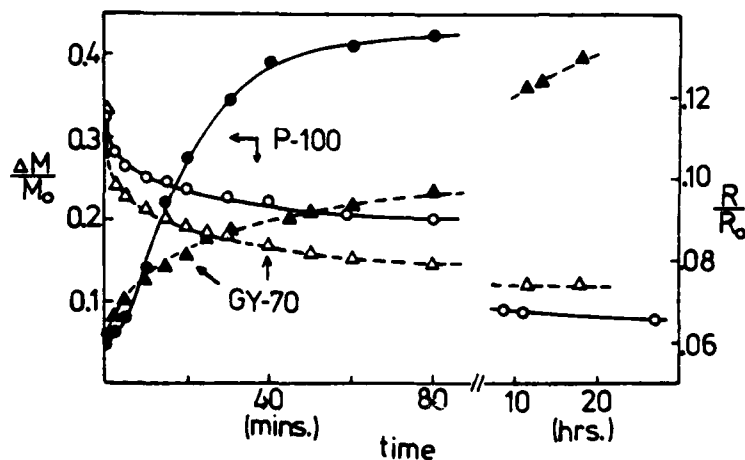


Figure 3. Weight ( $\circ, \Delta$ ) and resistance ( $\bullet, \blacktriangle$ ) changes on desorption in graphite fibers.

#### REFERENCES

1. Rudorff, W., *Z. Phys. Chem. B*, **45**, 42 (1939)
2. W. C. Forsman, F. L. Vogel, D. E. Carl, and J. Hoffman, *Carbon* **16**, 269 (1978)
3. D. E. Nixon, G. S. Parry, and A. R. Ubbelohde, *Proc. Roy. Soc. A*, **291**, 324 (1966)
4. J. E. Fischer, "Electronic Properties of Graphite Intercalation Compounds," Vol. 6, "Intercalated Layered Materials," F. Levy, ed., Reidel Publishing Co., Dordrecht, 1979
5. W. C. Forsman, F. L. Vogel, and D. E. Carl, *Mat. Sci. Eng.*, **47**, 187 (1981)
6. R. H. Perry, and C. H. Chilton, eds., "Chemical Engineers' Handbook," 5th ed., McGraw-Hill, 1973, p.3-66
7. C. Zeller, G. M. Foley, E. R. Falardeau, and F. L. Vogel, *Mat. Sci. Eng.* **31**, 255 (1977)
8. F. L. Vogel, *Fourth London Int'l. Conf. on Carbon and Graphite*, 332 (1974)
9. M. Dowell, *Ext. Abs. Prog.*, 13th Bienn. Conf. Carbon, 11 (1977)
10. M. Dowell, *Mat. Sci. Eng.*, **31**, 129 (1977)
11. J. A. Barker and R. C. Croft., *Aust. J. Chem.*, **6**, 302 (1953)
12. K. K. Bardhan and Chung, *Ext. Abs. Prog.*, 14th Bienn. Conf. Carbon, 282 (1979)
13. W. Metz and L. Siemsgluss, *Mat. Sci. Eng.*, **31**, 119 (1977)
14. J. Crank, "The Mathematics of Diffusion," 2nd ed., Oxford, 1975

[Appendix 5]

THE SYSTEM GRAPHITE -  $MnCl_2$  -  $AlCl_3$ :  
KINETICS, STRUCTURE AND MECHANISM OF FORMATION

T. Dziemianowicz\*, R. Vangelisti†, A. Herold†, and W. Forsman\*

\* Department of Chemical Engineering  
University of Pennsylvania  
Philadelphia, PA 19104

+ Laboratoire de Chimie Minerale Appliquee  
Universite de Nancy I  
C. O. 140  
54500 Vandoeuvre, France

Abstract

Graphite-MnCl<sub>2</sub>-AlCl<sub>3</sub> intercalation compounds have been prepared via MnCl<sub>2</sub>-AlCl<sub>3</sub> complexes using the two bulb technique. First stage compounds are eventually formed at both 325<sup>o</sup> and 500<sup>o</sup>C; products formed at the lower reaction temperature are richer in Mn (C<sub>5.95</sub>MnCl<sub>2</sub>(AlCl<sub>3</sub>)<sub>0.21</sub>) than those at 500<sup>o</sup> (C<sub>7.15</sub>MnCl<sub>2</sub>(AlCl<sub>3</sub>)<sub>0.3</sub>). At 325<sup>o</sup> the mechanism is a quasi-selective intercalation of AlCl<sub>3</sub> to the second stage followed by insertion of MnCl<sub>2</sub> to a mixed stage 1 compound, and finally an iso-stage Mn enrichment with Al depletion. The 500<sup>o</sup> reaction proceeds differently; some manganese dichloride is incorporated in the lattice at shorter reaction times, but further enrichment occurs slowly. Rate limiting reactions at each temperature are proposed.

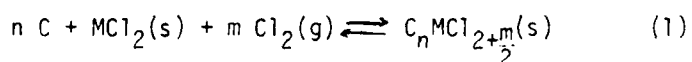
Powder x-ray diffractograms give  $I_c = 9.51 \text{ \AA}$  for Mn-rich first stage compounds. Comparison of calculated and observed (00 $\ell$ ) structure factors yields an Mn-Cl distance of 1.46  $\text{\AA}$  in the intercalant layer -- identical to that in the pure dichloride. X-ray spectra of products formed at 325<sup>o</sup> are rich in ( $hkl$ ) reflections, indicating long-range ordering of the intercalant. Analysis of ( $hkl$ ) positions and the (10 $\ell$ ) and (11 $\ell$ ) intensities of the inserted MnCl<sub>2</sub> indicate an intercalant superlattice with  $a_0 = 3.69 \text{ \AA}$  and  $c_0 = 3 \times I_c = 28.53 \text{ \AA}$ . The MnCl<sub>2</sub> domains have an estimated size of 120 $\text{\AA}$  in the a-axis direction. First stage compounds prepared at 500<sup>o</sup> have only ill-defined ( $hkl$ ) maxima and are thus less well-ordered.

Results obtained at 325<sup>o</sup>C are especially significant because (1) this represents the lowest temperature at which dichlorides have been intercalated to rich stages, (2) the reaction products have an apparent filling coefficient of unity and (3) long-range (i.e., three-

(1) this represents the lowest temperature at which dichlorides have been intercalated to rich stages, (2) the reaction products have an apparent filling coefficient of unity and (3) long-range (i.e., three-dimensional) ordering has been documented in a dichloride intercalation compound for the first time, and is sensitive to reaction temperature.

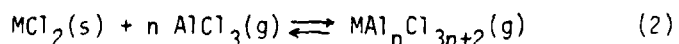
### Introduction

The insertion of transition metal dichlorides into the graphite lattice was heralded by Croft [1] in 1956. In the intervening quarter century, the list has grown considerably. A recent paper lists the chlorides of Cd, Co, Cu, Hg, Mn, Ni, Pd, and Zn as those known to intercalate in the presence of free chlorine [2]; FeCl<sub>2</sub> graphite intercalation compounds (GIC's) have also been prepared, but only by reduction of FeCl<sub>3</sub> compounds [3]. Because of their exceedingly low vapor pressures -- typically less than one torr at 500°C -- high reaction temperatures are required and rates of formation are slow. It appears, in fact, that this particular balance of thermodynamic and kinetic factors often precludes formation of rich (i.e., first stage) compounds. That is, at temperatures sufficient to give a measurable reaction rate, the intercalation-desorption equilibrium (eqn. 1) may be shifted to the left, allowing only formation of



dilute stage compounds. Nickel chloride, for example, is inserted only to the second stage, and the chlorides of mercury, palladium and zinc do not progress beyond stage three.

In 1977 Stumpp reported that the addition of AlCl<sub>3</sub> to transition metal dichlorides (CoCl<sub>2</sub>, NiCl<sub>2</sub>) or lanthanide trichlorides augments their rate of intercalation [4]. This effect was attributed to a well-known enhanced "apparent volatility" of the chloride due to complexation:



In this manner, non-volatile chlorides may be transported via vapor phase complexes. The increase in concentration of the metal, M, in the vapor phase is striking; the ratio of complex vapor pressure to that of the pure chloride at the same temperature may exceed  $10^{10}$ . The results of Stumpp's work are reproduced graphically in Figure 1. As the quantity of  $AlCl_3$  is increased its partial pressure and that of the complex must both rise (at  $500^\circ C$  all of the  $AlCl_3$  will be in the vapor phase):

$$P_{MA_1nCl_{3n+2}} = K_n [P_{AlCl_3}]^n \quad (3)$$

It can be seen in Fig. 1 that the reaction rate increases accordingly. But this interesting work raised more new questions than it solved. For example, can intercalation via  $AlCl_3$  complexes proceed at reduced temperatures, and if so, how low, and at what rate? And is it possible to produce richer compounds by this route than by direct combination of graphite and the dichloride?

In an earlier paper [5], we presented preliminary results on the system graphite- $MnCl_2$ - $AlCl_3$  which may be summarized as follows:

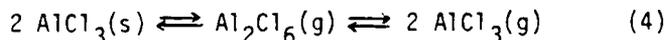
- a) synthesis - first stage compounds were prepared from natural graphite powders at temperatures as low as  $325^\circ C$ ; the richest compound prepared under these conditions had a composition by chemical analysis of  $C_{5.95}MnCl_2(AlCl_3)_{0.21}$
- b) mechanism - at  $325^\circ$ ,  $AlCl_3$  is first selectively intercalated to stage 2, after which  $MnCl_2$  enters the lattice. At  $500^\circ$  a different mechanism prevails
- c) structure - powder diffractograms indicate that the  $MnCl_2$  is

well-ordered in the  $325^\circ$  compound and retains the rhombohedral (ABC) stacking sequence which it possesses in the pure state. In a related study [2], it was shown that the (hk0) reflections are identical to those of an  $\text{MnCl}_2$  compound prepared via the direct synthesis, with the carbon and  $\text{MnCl}_2$  a-axes at a  $30^\circ$  angle to one another

In the present study, we present further data on this system, the interpretation of which permit a better understanding of the optimum reaction conditions, mechanism of insertion and structure of the equilibrium products. Where possible, results are compared with the very recent report of Baron, et al. [6] on  $\text{MnCl}_2$  GIC's prepared via the direct synthesis.

#### Experimental

Graphite- $\text{MnCl}_2$ - $\text{AlCl}_3$  compounds were prepared by the classic tube à deux boules technique. Ceylon graphite (particle size  $\leq 40\mu$ ) and in some cases thin pyrographite plaques ( $\sim 10 \times 2 \times 0.2$  mm) were placed in one end of the tube. The reagent portion of the tube contained anhydrous  $\text{MnCl}_2$  (as received) and anhydrous  $\text{AlCl}_3$  (resublimed); the amount of  $\text{AlCl}_3$  was measured so as to give a total initial pressure of about 4 torr, according to the equilibrium [7]



$$\log_{10} K(\text{mm}) = -6749/T - 2.013 \log_{10} T + 16.628$$

For kinetic experiments,  $\text{MnCl}_2$  was always present in excess of that requires to produce a first stage compound. Molar ratios of  $\text{AlCl}_3:\text{MnCl}_2$  were thus on the order of unity. It should be noted that physical mixing

of the graphite with intercalant was scrupulously avoided in order to avoid subsequent washing of the products, a common technique with other investigators. Reaction tubes were sealed under 500 torr  $\text{Cl}_2$  and placed in a two-zone furnace such that the graphite temperature always exceeded that of the chloride mixture ( $\Delta T = 25\text{-}50^\circ\text{C}$ ). On exiting the furnace, the reagent portion of the tube was quenched first to minimize the risk of condensing intercalant onto the graphite.

Products were weighed in a glove box under dry air to determine weight uptake ( $\Delta m/m_0$ ), and samples were analyzed for carbon, hydrogen, chlorine and metal content by the C.N.R.S. Service Central d'Analyse. Powder x-ray spectra were obtained by diffractometer (Mo  $K_\alpha$  radiation) in transmission with the sample sealed in a Mylar cellule. Pyrographite (00 $\bar{1}$ ) and ( $hk0$ ) scans were performed in similar fashion with samples sealed in glass capillaries.

## Results and Discussion

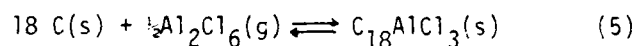
### A. Equilibrium products, kinetics and mechanism

Kinetic data (weight uptake vs. reaction time) are plotted in Figure 2 for compounds prepared from graphite powder at various reaction temperatures. The agreement between measured weight uptake and that calculated from analytical data (as (1-%C)/%C) is quite good. At both  $325^\circ$  and  $500^\circ\text{C}$ , rich products are eventually formed which appear to be pure first stage compounds according to their x-ray (00 $\bar{1}$ ) reflections. Surprisingly, reactions at  $400^\circ$  failed to yield a first stage compound. After 93 hrs., a mixture of stages 3 and 2 ( $\Delta m/m_0 = 80\%$ ) is formed, and at 209 hrs. a second stage compound is obtained ( $\Delta m/m_0 = 160\%$ ) with only

traces of the first stage. This observation is consistent with thermodynamic properties of the  $\text{MnCl}_2\text{-AlCl}_3$  system. Mass spectrometry data of Binnewies [10] show that substantial amounts of  $\text{MnAl}_2\text{Cl}_8$  and  $\text{MnAlCl}_5$  exist in the vapor phase at  $325^\circ$  and  $500^\circ\text{C}$  respectively, but that neither complex is as abundant at  $400^\circ$ . Thus it is not unreasonable that the reaction at  $400^\circ$  is a bit sluggish. Unfortunately, the data are insufficient to determine whether a first stage compound appears thermodynamically forbidden at  $400^\circ$  due to a low complex partial pressure, or if this merely poses a kinetic limitation.

#### Reaction at $325^\circ$

Figure 3 shows the evolution of the x-ray powder diffraction spectra of graphite- $\text{MnCl}_2\text{-AlCl}_3$  compounds prepared at  $325^\circ$  with the (001), i.e., staging lines indicated. In conjunction with the analytical data presented in Figure 4, the following pattern emerges. The graphite is first rapidly and selectively intercalated to stage 2 with  $\text{AlCl}_3$ . The ideal stoichiometry of this reaction,



compares favorably with the analytical result ( $\text{C}_{16.4}\text{AlMn}_{0.3}\text{Cl}_{3.6}$ ). This is followed by a regime during which Mn content increases at roughly constant Al content (Fig. 4) accompanied by a change in stage from 2 to 1. Finally, Mn content rises to its equilibrium value, but with Al depletion in a process which is iso-stage. It is noteworthy that at the longest reaction times, the total metal chloride content determined by chemical analysis exceeds the limiting compositions

$C_{4.5}MnCl_2$  and  $C_9AlCl_3$  for the richest pure component intercalation compounds<sup>†</sup>. There is, however, some evidence of adsorbed  $MnCl_2$  in the x-ray spectra. It is conceivable that after the intercalation compound becomes "saturated" with intercalant,  $MnCl_2$  continues to be transported via the vapor phase complexes, but finding no further vacancies within the lattice is forced to remain outside -- i.e., on the graphite surface.

Figure 5 depicts schematically two possible mechanisms which are consistent with these results. Both are conceptually similar, differing only in minor details. Mechanism II is based on the folded-sheet model of Daumas and Hérold [11]. After the formation of the stage 2 compound (a),  $MnCl_2$  is gradually added to the lattice -- initially filling the interlaminar spaces to give a mixed first stage compound (b). This step is consistent with the increase in Mn content -- which is manifest in both the analytical data (Fig. 4) and the growth of the  $MnCl_2$  (110) peak (Fig. 3) -- at constant Al level. As the proportion of Mn rises further, it can do so only at the expense of aluminum. In mechanism I this entails an exchange of the metal chlorides, probably mediated by  $MnAl_nCl_{3n+2}$  molecules at the edges of the graphite planes; in mechanism II the invading  $MnCl_2$  front effectively pushes the  $AlCl_3$  out of the lattice. Unlike the previous step, this process occurs at constant stage (no change in  $(00\bar{1})$  positions in the upper traces of Fig. 3). With some

<sup>†</sup>  $C_9AlCl_3$  is the commonly observed stoichiometry for saturated first stage aluminum chloride compounds. One arrives at a composition  $C_{4.5}MnCl_2$  by comparing the hexagonal lattice parameters,  $a$ , for graphite (2.46Å) and  $MnCl_2$  (3.68Å). The ratio of the areas of the hexagonal cells (projected perpendicular to the c-axis) is thus  $(3.68/2.46)^2 = 2.24$ . Since there are two carbon atoms per cell versus a single  $MnCl_2$  unit, this ratio must be doubled, thereby giving  $C/MnCl_2 = 4.5$ .

$\text{MnCl}_2$  now in every interlaminar space, consolidation and long-range ordering of the  $\text{MnCl}_2$  domains begins (c), signaled by the appearance of the (10 $\bar{l}$ ) and (11 $\bar{l}$ ) complexes on the x-ray pattern. Finally, only small islands of  $\text{AlCl}_3$  remain, either kinetically trapped at the interior of an intercalant layer, or perhaps ionically bound as  $\text{AlCl}_4^-$  -- either of these is a plausible explanation as to why it seems impossible to remove all of the aluminum from the lattice under these conditions, even at long reaction times.

Stepwise mechanisms such as this are not unheard of in the intercalation literature. Freeman<sup>4</sup> added  $\text{N}_2\text{O}_5$  to a dilute graphite-ferric chloride intercalation compound and obtained a ternary of reported composition  $\text{C}_{31}\text{FeCl}_3(\text{N}_2\text{O}_5)_{1.7}$ . Presumably the  $\text{N}_2\text{O}_5$  is inserted in the vacant interlaminar spaces, though no x-ray data are presented. Thallium halides will also undergo sequential insertion reactions. Stumpp [13] has shown that graphite-thallium bromide compounds which have a limiting composition of stage 2, may be reacted with  $\text{TlCl}_3$  to yield a mixed first stage compound  $\text{C}_{12.5}\text{TlCl}_{1.8}\text{Br}_{1.6}$ . The most directly analogous reaction, however, is that of the formation of the ternary donor compound  $\text{KHgC}_4$ . According to Lagrange, et al. [14], insertion proceeds as follows. When pyrographite is exposed to the saturated vapor of a  $\text{KHg}$  amalgam, potassium is selectively inserted first, progressing through weaker stages until stage 1  $\text{KC}_8$  is obtained (it is pointed out that this step is not *completely* selective; some mercury is soluble in the intercalated potassium sheets, just as there is some  $\text{MnCl}_2$  in the initial stage 2  $\text{AlCl}_3$  compound in the present work). In the second step, mercury and more potassium are inserted cooperatively to give the final product  $\text{KHgC}_4$ .

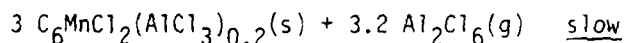
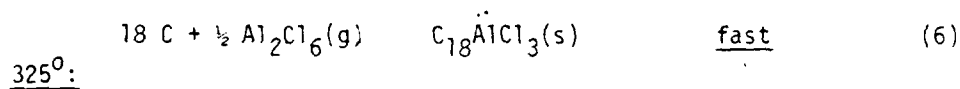
with its characteristic K-Hg-K trilayered intercalant. As in the  $\text{MnCl}_2$  reaction, this is an iso-stage process, though the interlayer spacing expands markedly from  $5.32\text{\AA}$  in  $\text{KC}_8$  to  $10.16\text{\AA}$  in  $\text{KHgC}_4$ .  $\text{AlCl}_3$  and  $\text{MnCl}_2$  layers, on the other hand, have nearly identical values of  $I_c$  -- about  $9.5\text{\AA}$ .

Further support for a sequential mechanism is provided by the following experiment. If, rather than using an excess of  $\text{MnCl}_2$ , the reactant mixture contains only enough of the dichloride to yield a second stage compound (calculated as  $\text{C}_9\text{MnCl}_2$ ), the results are as follows. At equilibrium, the  $\text{MnCl}_2$  appears to be completely consumed, x-ray (00 $\ell$ ) lines indicate a first stage compound, and chemical analysis gives  $\text{C}_{12.7}\text{MnCl}_2(\text{AlCl}_{2.6})_{0.85}$ . This corresponds well with a situation such as (b) in Fig. 5. All interlaminal spaces are filled, but with no further  $\text{MnCl}_2$  available, the mechanism is arrested at the mixed first stage.

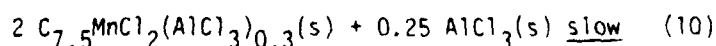
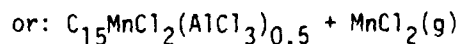
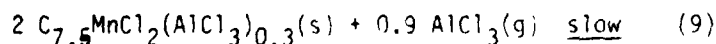
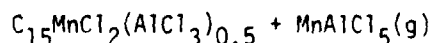
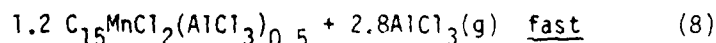
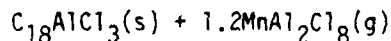
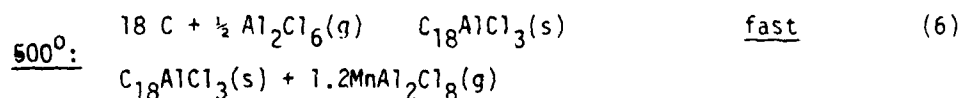
#### Reaction at $500^\circ\text{C}$

Stage evolution and compositional changes at  $500^\circ\text{C}$  are presented in Figs. 6 and 7 respectively. It is clear that insertion proceeds somewhat differently at higher temperature. Once again a stage 2 compound is formed at the outset, but unlike the reaction at  $325^\circ$ , significant quantities of manganese are present even at short reaction times. At 12 hrs. the manganese content is already comparable to that of the aluminum, and the (110) peak of the inserted  $\text{MnCl}_2$  is quite pronounced (compare the 12 hr. trace in Fig. 6 with that at 10 hr. in Fig. 3). Further enhancement of Mn content is quite slow; it is not until about eight days that

a first stage compound is finally observed. This is in contrast to the 325° case in which the Mn content rises more or less continuously after early formation of the stage 2 AlCl<sub>3</sub> system. These results are readily explained in terms of rate limiting reactions at each temperature. As mentioned previously, at 325° the rate of MnCl<sub>2</sub> insertion is governed by reaction via the gaseous complex MnAl<sub>2</sub>Cl<sub>8</sub>:



At 500°, the vapor phase consists of no fewer than six species. In approximate order of decreasing vapor pressures, these are Al<sub>2</sub>Cl<sub>6</sub>, Cl<sub>2</sub>, AlCl<sub>3</sub>, MnAlCl<sub>5</sub>, MnAl<sub>2</sub>Cl<sub>8</sub>, MnCl<sub>2</sub>. The early appearance of manganese in the reaction products probably reflects faster kinetics of reaction (7) at 500°. However, since the partial pressure of the MnAl<sub>2</sub>Cl<sub>8</sub> complex is lower at this temperature, the equilibrium is shifted to the left, and the product of that reaction is less rich in Mn than at 325°. Further insertion of MnCl<sub>2</sub> is subsequently limited by the rate of reaction with the MnAlCl<sub>5</sub> complex -- or by the faint pressure of MnCl<sub>2</sub>:



b) Structure of graphite-MnCl<sub>2</sub>-AlCl<sub>3</sub> compounds

c-axis ordering

First stage compounds gave values of 9.51<sup>0</sup>Å for I<sub>c</sub>, the c-axis repeat distance. This is identical to that reported by Stumpp and Werner [8] in the earliest study of an MnCl<sub>2</sub> GIC, but slightly larger than found recently by Baron, et al. [6]. It must be remembered, however, that the initial presence of AlCl<sub>3</sub> in the lattice could have had some bearing on the later structure.

Analysis of the (00l) reflections was carried out as follows. Stoichiometry was first adjusted to take into account adsorbed MnCl<sub>2</sub>. If ratios C:AlCl<sub>3</sub>=9 and C:MnCl<sub>2</sub>=4.5 are assumed, and all AlCl<sub>3</sub> is taken to be present inside the lattice (condensation is unlikely at 325<sup>0</sup>) then maximum filling of the graphite occurs at a composition of C<sub>6</sub>(MnCl<sub>2</sub>)<sub>0.91</sub>(AlCl<sub>3</sub>)<sub>0.21</sub> with about 9% adsorbed material. With the stoichiometric coefficients n<sub>i</sub> thus determined, the single remaining unknown is z\* -- the dimensionless distance between Mn and Cl layers -- and B, the Debye temperature factor

$$\begin{aligned} F_{00l} &= \exp(-B \sin^2 \theta / \lambda^2) \sum_i n_i f_i \cos(2\pi l z_i) \\ &= \exp(-B \sin^2 \theta / \lambda^2) \{ 0.21 f_{Al} + 0.91 f_{Mn} + 6 f_C \cos \pi l \\ &\quad + f_{Cl} (0.63 \cos(.294 \pi l) + 1.82 \cos 2 - \pi l z^*) \} \quad (11) \end{aligned}$$

The Al-Cl distance was assumed to be 1.40<sup>0</sup>Å as determined by Leung, et al. [9] (alternatively, one could treat all Cl atoms as identical, separated by a single distance from the plane of Mn and Al atoms; in this work, results for both approaches were identical). Simultaneous solution for z\* and B was accomplished by minimizing the residue

$$R = \frac{\sum |F_{00l}| - |F_{00l,obs}|}{\sum |F_{00l,obs}|} \quad (12)$$

The minimum value of R is 0.20 and occurs at  $z^*=0.153$  with  $B=2.9\text{\AA}^2$ ; calculated and observed structure factors for these conditions are listed in Table 1. This value of  $z^*$  corresponds to an Mn-Cl distance of  $1.46\text{\AA}$  -- the same as observed in pure  $\text{MnCl}_2$ , but slightly greater than that reported by Baron, et al. [6]. The small number of reflections and possibility of interference with  $(hkl)$  peaks probably account for the relatively high R value. It is curious that Baron et al. found a contracted spacing accompanied by a fairly large degree of charge transfer. Mutual repulsion of negatively charged chlorine layers would more likely favor expansion; this is indeed observed in the  $\text{AlCl}_3$  system [9] at an even lower level of charge transfer.

#### Long-range order

The abundance of  $(hkl)$  reflections in the powder diffractograms of compounds prepared at  $325^\circ$  (top of Fig. 2) suggests long-range -- i.e., three-dimensional ordering--of the  $\text{MnCl}_2$  layers. In pure  $\text{MnCl}_2$ , Cl-Mn-Cl trilayers are stacked in a rhombohedral A-B-C sequence. The corresponding structural parameters are  $a_0=3.68\text{\AA}$  and  $c_0=17.47\text{\AA}$ , with the atomic positions in the cell given by

$$\text{Mn: } 000; rh \quad \text{Cl: } 00u, 00\bar{u}; rh \quad (13)$$

where  $u \sim 0.25$  for many substances with the  $\text{CdCl}_2$  structure [15].

Structure factors for  $(10l)$  and  $(11l)$  reflections calculated from

$$F_{hkl} = \sum_n f_n \exp(2\pi i(hx_n + ky_n + lz_n)) \quad (14)$$

are listed in Table 2 with observed structure factors obtained by diffractometer with Mo K radiation and after correction by Lorentz-polarization factors. After intercalation the  $\text{MnCl}_2$  (110) reflection gives a slightly lengthened value of  $a_0$  --  $3.69\text{\AA}$ . If the  $\text{MnCl}_2$  superlattice has retained its A-B-C stacking on insertion, the c-axis parameter will have increased to  $c_0 = 3 \times I_c = 28.53\text{\AA}$ . Furthermore, the parameter  $u$  (eqn. 13), which enters into  $(hkl)$  structure factor calculations, would be changed from 0.25 to 0.283, assuming an Mn-Cl distance of  $1.46\text{\AA}$  as deduced in the last section. Hence, both the positions and magnitudes of the  $F_{hkl}$  would change in a predictable way on insertion. Observed  $(hkl)$  positions in Mn-rich stage 1 compounds coincide exactly with calculated values of  $d_{hkl}$  using  $c_0 = 28.53\text{\AA}$ .

Table 3 lists calculated and experimental structure factors for the (10 $\bar{2}$ ) and (11 $\bar{2}$ ) reflections. As predicted, the (107) peak has grown to equal the magnitude of the (104) (compare with Table 2 for pure  $\text{MnCl}_2$ ). And in the (11 $\bar{2}$ ) reflections, although observed magnitudes are slightly higher than calculated, the ratios  $F_{110}:F_{113}:F_{116}:F_{119}$  are in close agreement, and fall off less sharply than in pure  $\text{MnCl}_2$ . Using the method of Stokes and Wilson [16], the breadth of the  $\text{MnCl}_2$  (110) reflection gives a crystallite size of  $120\text{\AA}$  in the a-axis direction for the intercalated  $\text{MnCl}_2$  lattice; this echoes the findings of Baron, et al. in their study of the direct synthesis of  $\text{MnCl}_2$  compounds (Ceylon graphite was also used in that study). It is interesting that Mn-rich first stage compounds prepared at  $500^\circ$  yield much less well-defined  $(hkl)$  maxima; structural disorder at elevated reaction temperatures has also been reported for the direct synthesis [6].

### C) Results with Pyrographite

Characterization of pyrographite products was less definitive than that of powders. Due to small sample size, chemical analyses were not feasible and weight uptake measurements would have been accompanied by a high degree of uncertainty. Diffractometer scans of (00 $l$ ) and ( $hk0$ ) reflections did, however, provide some information. At 325 $^{\circ}$ , the mechanism begins as in powders; at short times the (00 $l$ ) positions and intensities are those of stage 2 AlCl $_3$  with no discernible MnCl $_2$  (110) reflection. After several days a stage 1 compound is formed. Unlike powder samples, however, the (00 $l$ ) intensities are intermediate between those of a first stage AlCl $_3$  and MnCl $_2$  (for pure MnCl $_2$  compounds, the (002) is most intense, whereas in AlCl $_3$  it is the (003)), and the ( $hk0$ ) reflections (Figure 8) include both a strong MnCl $_2$  (110) and weak reflections at lower angles which are identical to those found in pure AlCl $_3$  GIC's [17]. Thus, even at long reaction times, the AlCl $_3$  concentration in pyrographite products is sufficient to alter (00 $l$ ) intensities and to produce domains with in-plane ordering. The breadth of the sharpest AlCl $_3$  ( $hk0$ ) reflection (at  $\sim 4^{\circ}$ ) indicates that the AlCl $_3$  domains are about half the size of those for MnCl $_2$  -- i.e., on the order of 50 $\text{\AA}$ .

### Conclusions

First stage compounds graphite- $\text{MnCl}_2$ - $\text{AlCl}_3$  have been prepared at  $325^\circ$  and  $500^\circ\text{C}$  via vapor phase complexes. This synthetic technique allows formation of rich stage metal dichloride compounds at the lowest temperature yet reported. Furthermore, transport of the chloride via vapor phase complexes obviates the need to physically mix the reactants -- a technique which requires subsequent washing of reaction products prior to characterization (a procedure which may leach intercalant from the edges of the interlaminar spaces [18]). Baron, et al. cite "filling coefficients" of 80-85% for first stage metal chloride compounds after an HCl wash. Results presented herein indicate that apparent filling coefficients of unity have been achieved in  $325^\circ$  compounds. If the  $\text{MnCl}_2$  does indeed form islands as proposed for other dichlorides [19,6], it is possible that the mobile  $\text{AlCl}_3$  molecules fill the interstices between islands, thus creating a very densely packed intercalant layer.

The mechanism of insertion at  $325^\circ$  is a quasi-selective intercalation of  $\text{AlCl}_3$  to stage 2, followed by  $\text{MnCl}_2$  addition to a mixed first stage and then iso-stage  $\text{MnCl}_2$  enrichment. The reaction at  $500^\circ$  proceeds differently, probably reflecting changes in the concentrations of the various species present in the vapor phase. Rate limiting reactions at both temperatures have been proposed to explain differences in kinetic and compositional data.

Three-dimensional ordering of the intercalant takes place at the lower reaction temperature but is less evident at  $500^\circ\text{C}$ . The  $\text{MnCl}_2$  retains its A-B-6 stacking on insertion, giving rise to an hexagonal lattice with parameters  $a_0 = 3.69\text{\AA}$  and  $c_0 = 3 \times I_c = 28.53\text{\AA}$ . Positions of numerous ( $h, k, l$ ) lines support this structural hypothesis, as do structure factor calculations for the (10 $l$ )

and (11 $\bar{L}$ ) reflections of the intercalated MnCl<sub>2</sub> lattice. This is the only report of three-dimensional ordering in a dichloride GIC and again is attributed to the lowered reaction temperatures which are only feasible through complexation.

Finally, this work sheds new light on the merits of Stumpp's initial report of intercalation via AlCl<sub>3</sub> complexes. Production of rich stages at greatly reduced temperatures is a significant practical advantage of this reaction pathway; formation of well-ordered compounds is an additional bonus for the intercalation scientist, and makes this technique an attractive one for future studies of dichloride intercalant systems.

#### Acknowledgment

This work was supported by the U.S. Army Research Office through Grant Number DAAG29-79-C-0208.

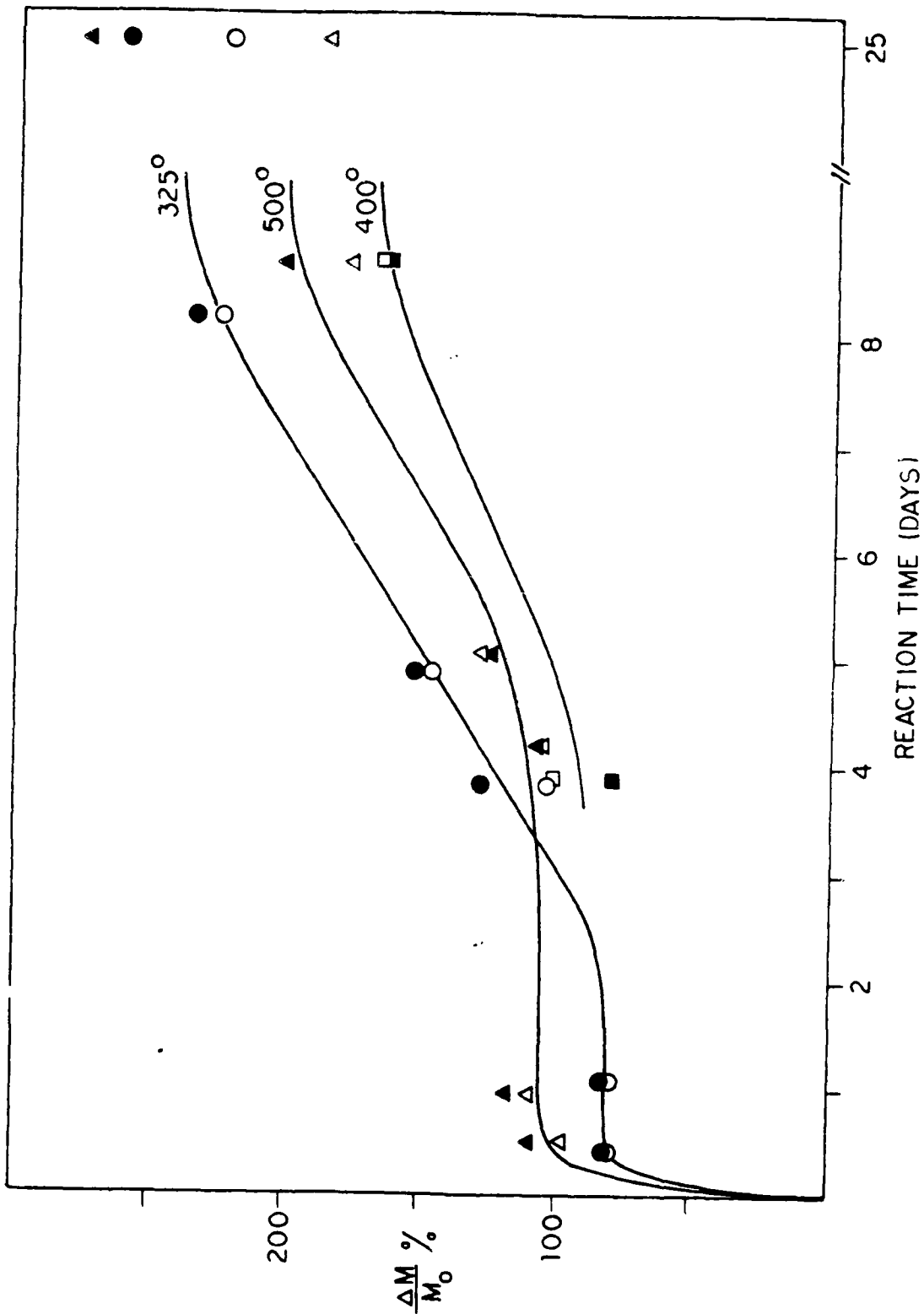
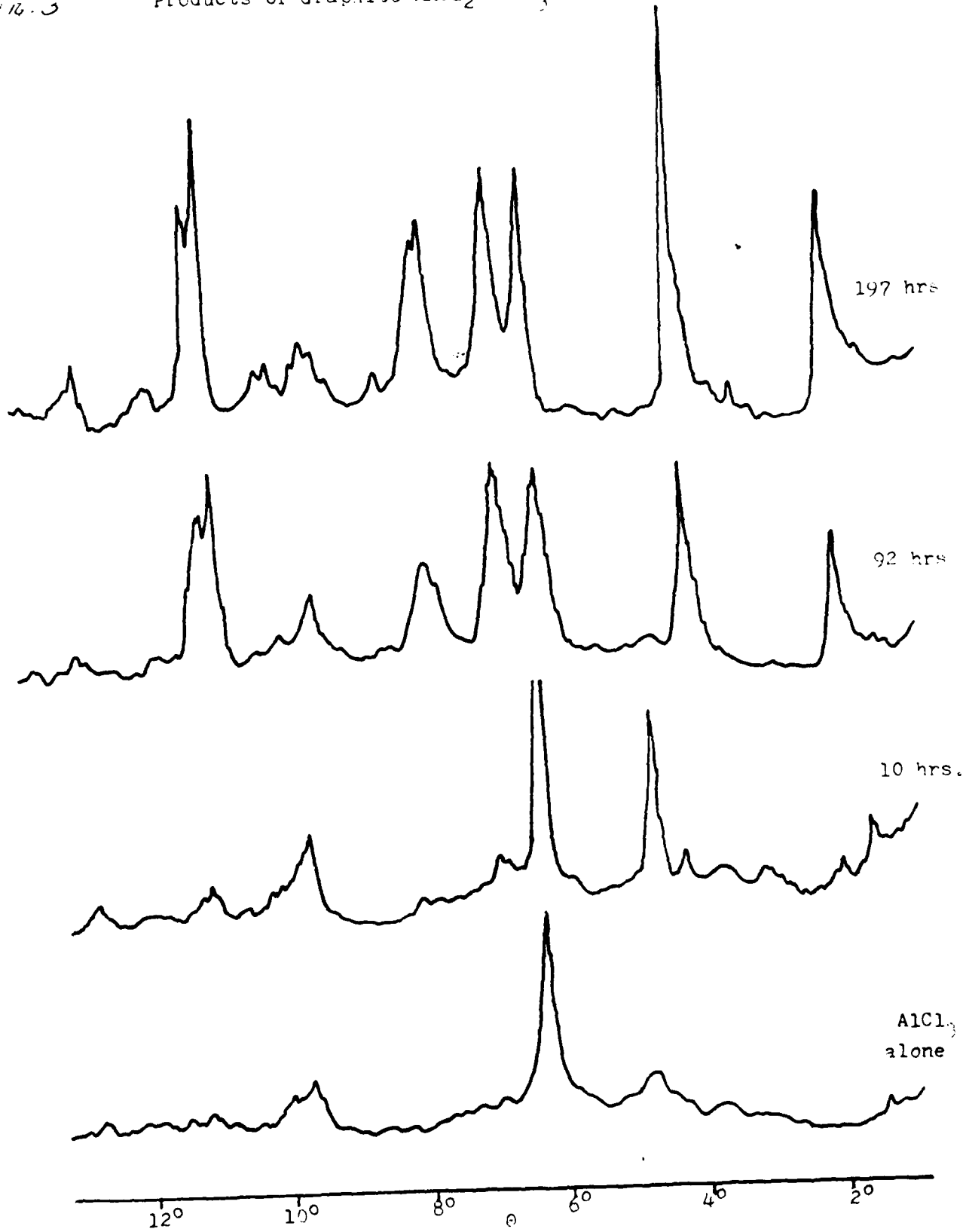
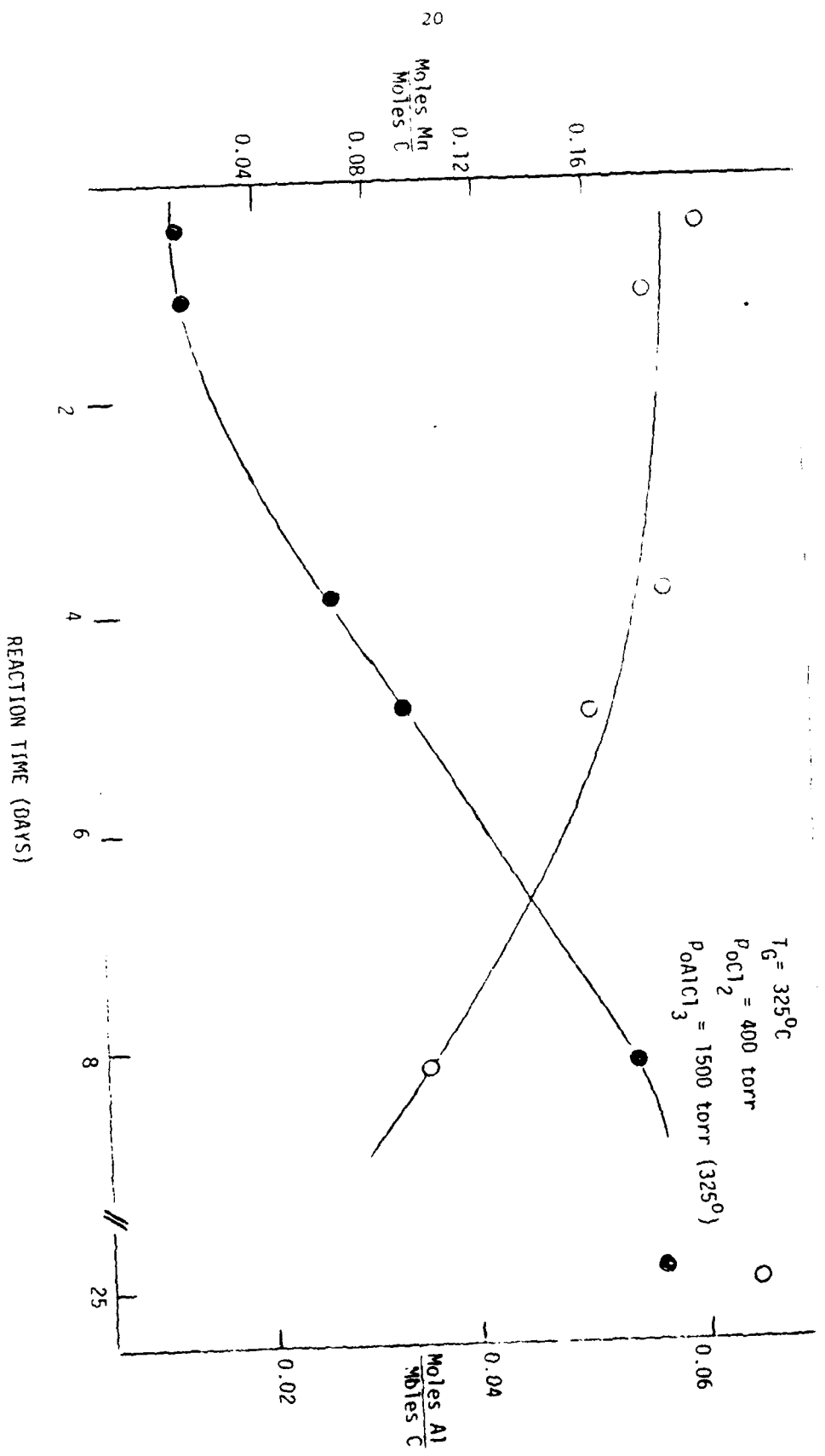


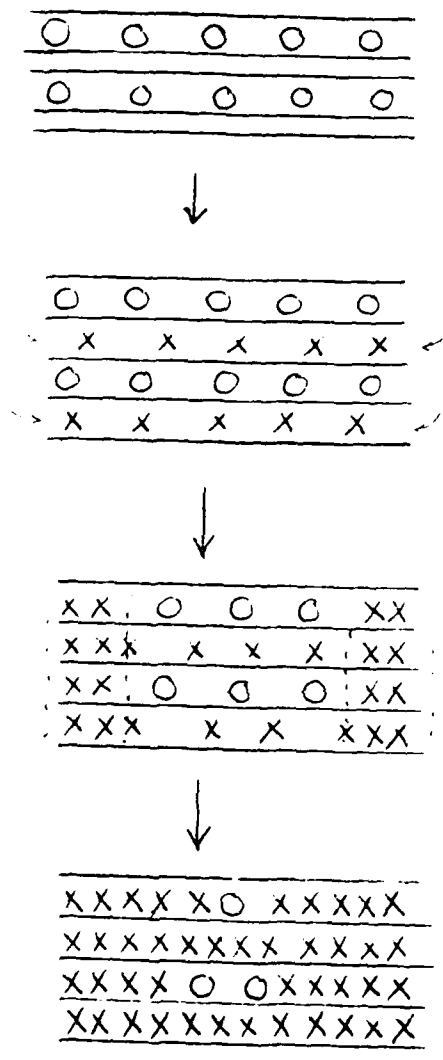
Figure 1. Change in mass of  $\text{MgO}$  as a function of reaction time at different temperatures. (O,  $\text{MgO}$ ;  $\Delta$ ,  $\text{MgO}$ ;  $\bullet$ ,  $\text{MgO}$ ;  $\blacktriangle$ ,  $\text{MgO}$ ;  $\square$ ,  $\text{MgO}$ ).

116.5

19  
Products of Graphite- $\text{MnCl}_2$ - $\text{AlCl}_3$  reaction at  $125^\circ\text{C}$

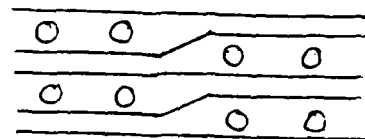




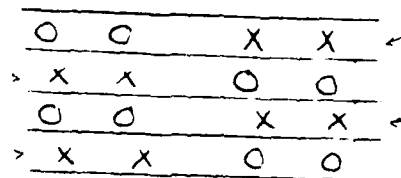


MECHANISM I

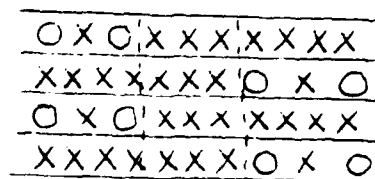
a. STAGE II  $AlCl_3$



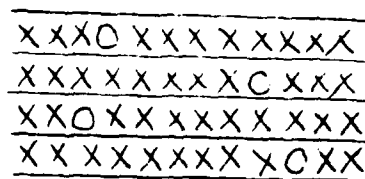
b. MIXED STAGE I



c. ORDERING OF  $MnCl_2$  DOMAINS



d. STAGE I  $MnCl_2$ ,  $AlCl_3$ , IMPURITIES



MECHANISM II

FIGURE 5

Fig. 6 Products of Graphite- $\text{MnCl}_2$ - $\text{AlCl}_3$  Reaction at  $500^\circ\text{C}$

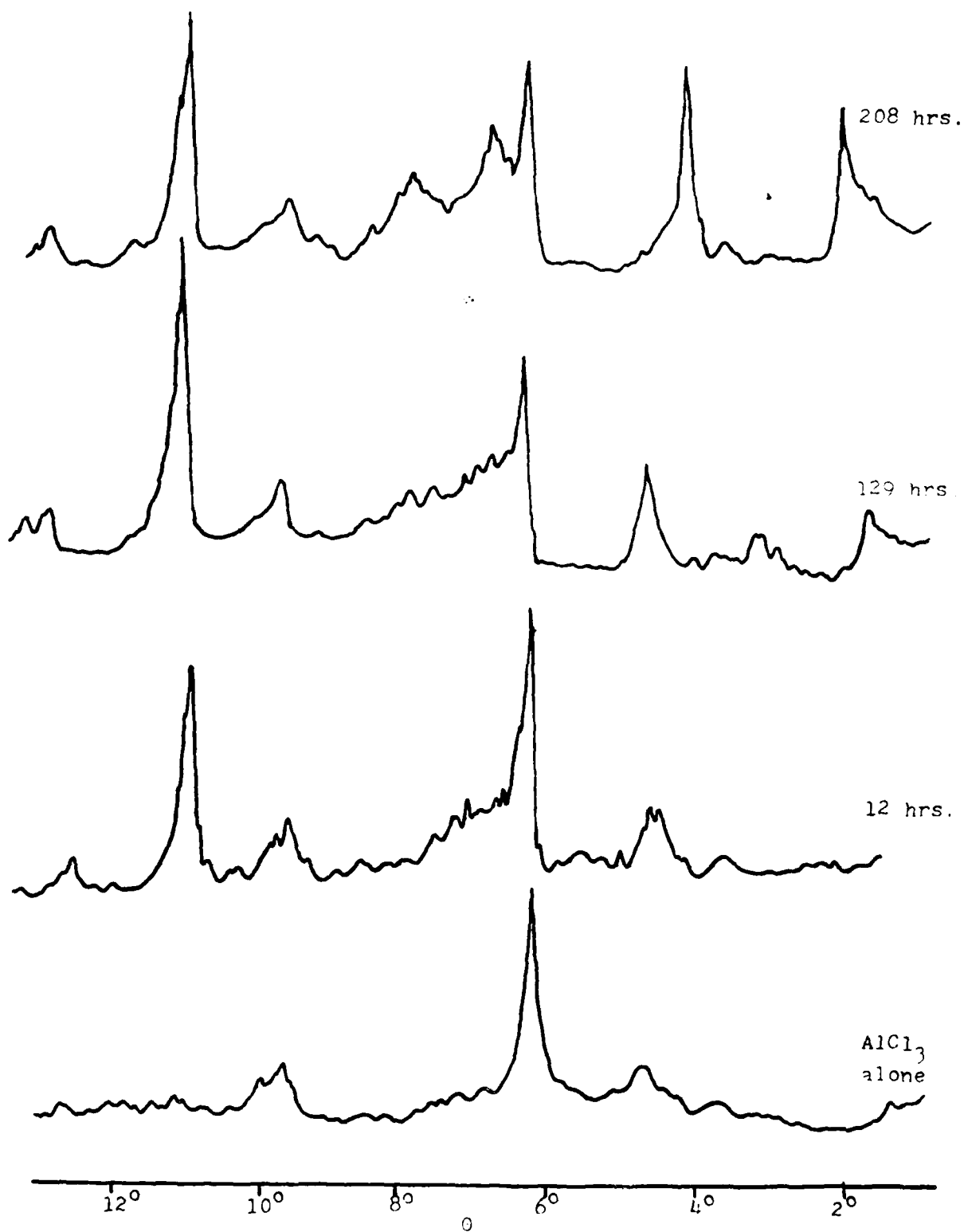


Fig. 7

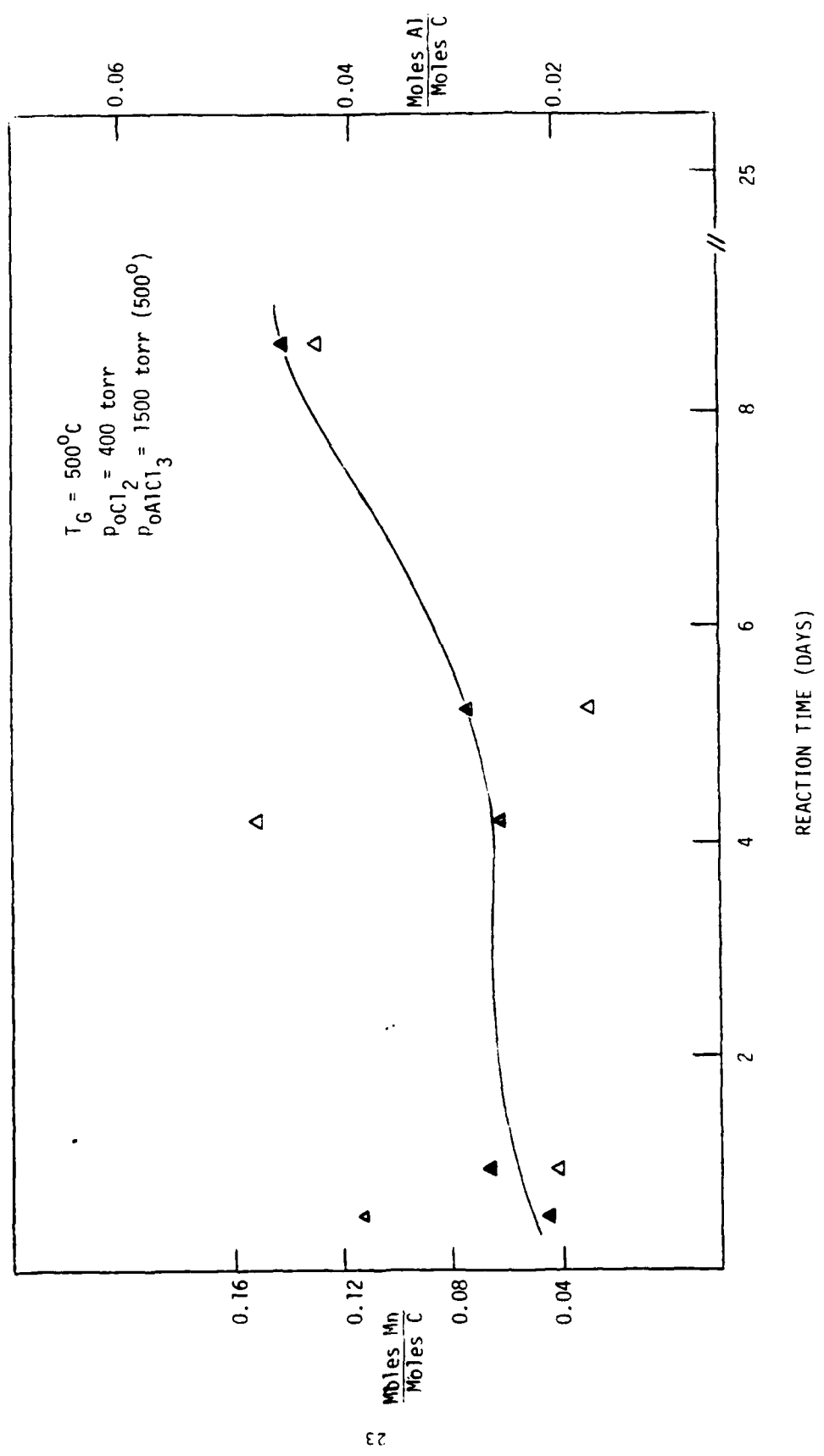
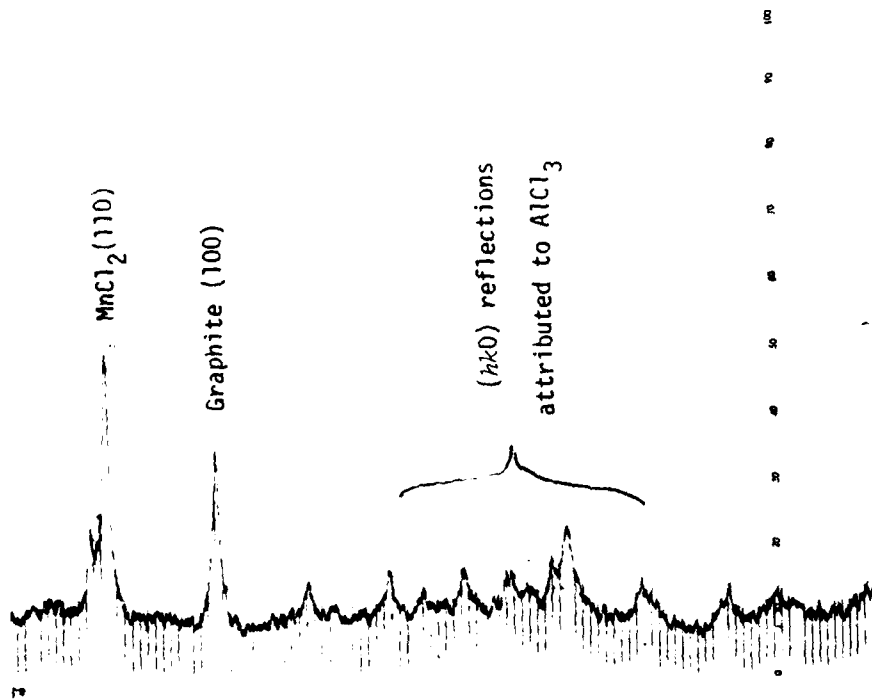


Fig. 6  
(XRD) DIFFRACTION PATTERN OF 40 MWCNT-ALCl<sub>3</sub> TEMPS



00l	I <sub>obs.</sub>	F <sub>obs.</sub>	F <sub>calc.</sub>
001	589	11.17	12.98
002	1000	-38.18	-38.15
003	711	41.13	34.72
004	190	15.03	14.93
005	n.o.		
006	240	29.42	36.69
007	41	6.02	14.05
008	161	27.80	17.22

Fit gave  $R=0.20$  with  $B=2.9\text{\AA}^2$

and  $d_{\text{Mn-Cl}} = 1.456\text{\AA}$

*Table 1*

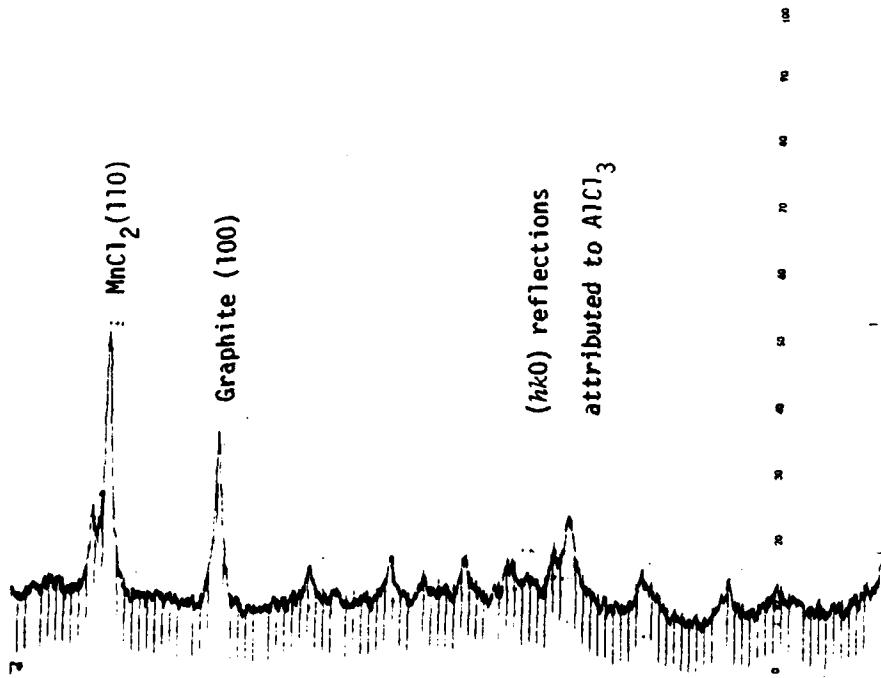
STRUCTURE FACTOR CALCULATIONS  
FOR PURE  $\text{MnCl}_2$

$(hkl)$	$d_{hkl}^0$ (Å)	$F_{\text{calc}}$ (arb. units)	$F_{\text{obs}}$ (arb. units)
(101)	3.15	$3f_{\text{Mn}}$ 47	50
(104)	2.58	$3f_{\text{Mn}} + 6f_{\text{Cl}}$ 100	100
(107)	1.97	$3f_{\text{Mn}}$ 40	44
(110)	1.84	$3f_{\text{Mn}} + 6f_{\text{Cl}}$ 85	91
(113)	1.76	$3f_{\text{Mn}}$ 38	59
(116) (202)	1.56	$3f_{\text{Mn}} - 6f_{\text{Cl}}$ -13	-21
(119)	1.34	$3f_{\text{Mn}}$ 31	32

STRUCTURE FACTOR CALCULATIONS  
FOR INTERCALATED  $\text{MnCl}_2$

$(hkl)$	$d_{hkl}(\text{\AA})$	$F_{\text{calc}}$ (arb. units)	$F_{\text{obs}}$ (arb. units)	
(101)	3.18	$3f_{\text{Mn}} - 1.22f_{\text{Cl}}$	34	*
(104)	2.94	$3f_{\text{Mn}} + 4.11f_{\text{Cl}}$	88	91
(107)	2.55	$3f_{\text{Mn}} + 5.94f_{\text{Cl}}$	100	100
(110)	1.85	$3f_{\text{Mn}} + 6.00f_{\text{Cl}}$	85	104
(113)	1.82	$3f_{\text{Mn}} + 3.45f_{\text{Cl}}$	65	89
(116)	1.72	$3f_{\text{Mn}} - 2.03f_{\text{Cl}}$	24	44
(119), (021), (202)	1.60	$3f_{\text{Mn}} - 5.79f_{\text{Cl}}$	27	34

\* Coincides with intense (00 $l$ ) reflection



References

1. R. Croft, Aust. J. Chem., 9, 184 (1956)
2. R. Vangelisti, and A. Herold, Ext. Abs. Proc., 15th Bienn. Conf. Carbon, 381 (1981)
3. B. Liegme, M. Bartlett, J. Hooley, and J. Sams, Phys. Letters, 25A, 127 (1967)
4. E. Stumpp, Mat. Sci. Eng., 31, 53 (1977)
5. T. Dziemianowicz, R. Vangelisti, W. Forsman and A. Herold, Ext. Abs. Proc., 15th Bienn. Conf. Carbon, 379 (1981)
6. F. Baron, S. Flandrois, C. Hauw and J. Gaultier, Solid State Comm., 42, 759 (1982)
7. E. Dewing, Metal. Trans., 1, 2169 (1970)
8. E. Stumpp, and F. Werner, Carbon, 4, 538 (1966)
9. S. Leung, M. Dresselhaus, C. Underhill, T. Krapchev, G. Dresselhaus and B. Wuensch, Phys. Rev. B, 24, 3505 (1982)
10. M. Binnewies, Z. Anorg. Allg. Chem., 437, 25 (1977)
11. N. Daumas and A. Herold, C. R. Acad. Sci. Paris, Ser. C, 268, 373 (1969)
12. A. Freeman, J. C. S. Chem. Comm., 746 (1974)
13. E. Stumpp, Carbon, 16, 259 (1978)
14. P. Lagrange, M. ElMakrini, D. Guerard, and A. Herold, Synth. Metals, 2, 191 (1980)
15. B. Warren, "X-ray Diffraction," Addison-Wesley, Reading, MA, 1969
16. R. Wyckoff, "Crystal Structures," Vol. 1, Interscience, New York, 1963
17. R. Vangelisti, unpublished results

[Appendix 6]

ACCEPTOR INTERCALATED GRAPHITE FIBERS:  
KINETICS, PRODUCT STABILITY AND APPLICATIONS TO COMPOSITES

T. S. Dziemianowicz\* and W. C. Forsman  
Department of Chemical Engineering  
University of Pennsylvania  
Philadelphia, PA 19104

SUMMARY

Kinetics of the intercalation of nitric acid in GY-70 (PAN-based) and P-100 (pitch) fibers have been analyzed using a two parameter nucleation/penetration model. Both the characteristic nucleation and penetration times --  $\tau_N$  and  $\tau_D$  respectively -- are longer in GY-70 than in P-100;  $\tau_N$  decreases with increasing  $p_{\text{HNO}_3}$ , while  $\tau_D$  remains constant. Staging is observed in both fiber types, with stages 2,3, and 4 observed in this study. The  $\alpha \rightarrow \beta$  phase transition has also been observed in a stage 4 P-100 fiber which was desorbed in air. Resistance measurements indicate that oxidation is completed fairly early in the overall reaction, as in HOPG, but desorption of neutrals from the equilibrium product adversely affects electronic properties, unlike HOPG. Stability of the desorbed fibers is also discussed.

P-100 fibers are readily intercalated with  $\text{AlCl}_3$  to give rich ( $\Delta m/m_0 = 128\%$ ) blue-black first stage compounds, whereas GY-70 intercalates  $\text{AlCl}_3$  to stage 2 ( $\Delta m/m_0 = 65\%$ ).  $\text{FeCl}_3$  is inserted with considerably more difficulty in both fiber types, leading to mixed stage compounds. All trichloride intercalated fibers studied are rapidly hydrated on exposure to ambient air.

Intercalated fiber composites (3% nitrate after desorption) have significantly better electrical properties than their pristine fiber counterparts, with no loss of mechanical integrity as measured by interlaminar shear strength. Future composite studies will be directed toward greater intercalant contents and accelerated aging experiments.

ACCEPTOR INTERCALATED GRAPHITE FIBERS:  
KINETICS, PRODUCT STABILITY AND APPLICATIONS TO COMPOSITES

T. S. Dziemianowicz<sup>\*</sup> and W. C. Forsman  
Department of Chemical Engineering  
University of Pennsylvania  
Philadelphia, PA 19104

1. INTRODUCTION

One of the most challenging problems facing researchers in the field of graphite intercalation is the conversion of graphite intercalation compounds (GIC's) into useful engineering materials. It has been shown that certain GIC's may be attractive candidates for battery materials[1], while others show promise as fluorinating agents in chemical synthesis[2]. At this point, however, so little is known of processing parameters and long-term material stability that implementation of these ideas is still a thing of the future. Graphite fibers, on the other hand, are already a viable commercial entity, and the enhancement of their physical properties through intercalation could render them even more attractive, especially in EMI shielding critical applications. Though intercalated carbon fibers have been known for some twenty years[3], little attention has been paid to reaction kinetics or stability of the products. The objective of the present work is to study intercalation behavior (kinetics and reaction products) of various graphite fibers with acceptor-type intercalants, to look at the stability of intercalated and desorbed fibers, and finally to obtain preliminary property data on intercalated fiber composites.

2. EXPERIMENTAL

The graphite types studied were HOPG, a PAN-based fiber (Celanese GY-70), and a pitch based fiber (Union Carbide P-100, VS-0054); sample preparation and nitric acid intercalation techniques have been described in detail elsewhere[4,5]. Trichloride intercalations were performed via the conventional

two-bulb method using the resublimed anhydrous chloride, and in the case of  $AlCl_3$ , 0.5 atm. of  $Cl_2$ . Composite fabrication has been described elsewhere [6,7]. Debye-Scherrer patterns of fibers were obtained with the fiber axis perpendicular to the incident beam ( $CuK\alpha$ ), thus accentuating (001) reflections. Samples were sealed in glass capillaries. Single fiber resistances were measured by a four-point technique[8]; composite resistances were obtained in similar fashion, using a jig comparable to that specified in ASTM D3355-74. Interlaminar shear strength (ILSS) was determined on a model TM Instron according to ASTM D2344-72.

### 3. RESULTS AND DISCUSSION

#### 3.1 Nitric acid intercalation

##### 3.1.1 Kinetics and equilibrium products

A new model for intercalation kinetics has recently been proposed, which includes the effects of both nucleation of the interlaminar spaces and intralayer growth[4]. Unlike earlier kinetic models based on simple diffusion of the intercalant[9], this approach incorporates a second mass transfer resistance -- that of nucleation -- as a time-dependent boundary condition. This approach is justified by a large body of data which suggest that nucleation proceeds sequentially from the outermost carbon planes [10,11]. The resulting expression for the normalized weight uptake is

$$\frac{M(t)}{M_\infty} = 1 - \frac{2J_1(\theta^{1/2})}{\theta^{1/2}J_0(\theta^{1/2})} e^{-t/\tau_N} + 4 \sum_{n=1}^{\infty} \frac{\exp(-c_n^2 t/\tau_D)}{c_n^2 (\frac{c_n}{\theta} - 1)} \quad (1)$$

where  $\tau_N$  and  $\tau_D$  are characteristic times for nucleation and intralayer penetration, respectively, and  $\theta$  is their ratio,  $\tau_D/\tau_N$ . It is easily verified that for diffusion controlled kinetics ( $\tau_D/\tau_N \gg 1$ ), equation (1) reduces to

the simple diffusion model, whereas in the nucleation controlled case ( $\tau_D/\tau_N \ll 1$ ), the result is analagous to that proposed by Metz and Siemsgluss [12].

In the initial report, it was shown that this model can be fit quite well to kinetic data for  $\text{HNO}_3$  intercalation of HOPG and graphite powder. It is especially significant that sigmoidal kinetic curves can be generated, whereas other models are always concave to the time axis and thus are incapable of reproducing so-called induction phenomena. In Figures 1 and 2, kinetic data for nitration of fibers are presented along with best fits of eqn. (i); parameters of the model are summarized in Table 1. Despite the considerably more complicated morphology of the fibers, the model is fairly successful at moderate  $\text{HNO}_3$  pressures. In GY-70 fibers, threshold effects apparently dominate for  $p_{\text{HNO}_3} \lesssim 10$  torr. In all of the P-100 fiber experiments, induction effects - the initial convex portion of the curve -- are more pronounced than in GY-70. Again, below 10 torr of  $\text{HNO}_3$  pressure the model is unsatisfactory, although intercalation ultimately proceeds to a much greater extent than in GY-70 at these conditions. It can be seen that the primary effect of lowering  $p_{\text{HNO}_3}$  is to increase the nucleation time (Table 1). It would be interesting to see if decreasing  $T_G$  at constant  $p_{\text{HNO}_3}$  slows kinetics instead by increasing  $\tau_D$ . It is unrealistic to attempt to relate  $\tau_N$  and  $\tau_D$  to fiber characteristics such as dimensions, given the limited experimental base thus far and the complex nature of the graphite fibers. The point is that the model can indicate to what extent intercalation is nucleation or penetration controlled, and -- with some limitations -- is applicable to many different graphite types.

Finally, it is interesting to note that resistance measurements carried out in parallel with weight uptake show that, as in HOPG, electrical property changes are essentially complete at about half of the equilibrium weight

uptake (Figure 3). This suggests that in the mechanistic scheme proposed by Forsman, et al. [5], most of the oxidative (charge transfer) interactions are completed early in the reaction.

Stages 2-4 have been identified in the nitrated fiber by x-ray diffraction (Table 2). The presence of weak secondary (00l) reflections in both fiber types is suggestive of c-axis stacking as proposed by Nixon, et al. [13], though such assignments must be considered only tentative at this point. This would be especially surprising result in GY-70, since the pristine fiber appears to be completely turbostratic.

### 3.1.2 Desorption behavior and stability of desorbed fibers

The desorption behavior of  $\text{HNO}_3$  intercalated graphites has been discussed previously 4. For fibers, results may be summarized as follows:

- 1) little loss of intercalant can be induced except under vacuum
- 2) rich (stage 2,3) compounds may ultimately lose 75-80% of intercalant. Thus, maximum residual nitrate in a stage 2 compound is 8-10%.
- 3) electrical resistance increase monotonically with weight loss on desorption, up to about twice its initial value.

The last point is especially significant, in that it is possible to withdraw fully 50% of the intercalated nitric acid from HOPG with no adverse effects on electrical properties. In the case of HOPG, desorption is accompanied by successive stage changes, whereas in fibers, the desorbed product is a poorly ordered mixture of the original stage, more dilute stages and graphite. This loss of structural integrity may play an important role in the deterioration of electrical properties.

Surprisingly, environmental stability of desorbed fibers is not significantly better than when freshly intercalated (Figure 4). Thermal stability is improved, however. The amount of intercalant subsequently lost during thermogravimetric analysis (TGA) decreases, and the temperature of maximum

rate of weight loss is successively higher with more desorption. The  $\alpha \rightarrow \beta$  phase transition has also been observed, as a result of spontaneous desorption in air of a stage 4 P-100 fiber [7].

3.2 Trichloride intercalated fibers

Intercalation of metal trichlorides in graphite fibers has received attention only recently. Hooley found that PAN-based fibers reacted with  $AlCl_3$  to a composition  $C_{14}AlCl_3$ , but that  $FeCl_3$  formed only dilute compounds ( $\sim C_{71}FeCl_3$ ) [14]. More recently,  $AlCl_3$  and  $FeCl_3$  were intercalated in PAN and pitch based fibers, but no evidence of staging was found [15]. Transition metal dichlorides have also been inserted [16], with notable success in the case of  $AlCl_3$  facilitated reactions with Endo's benzene vapor fibers as a substrate [17]. In the present study, it was found that both  $AlCl_3$  and  $FeCl_3$  intercalation compounds of graphite fibers demonstrate typical staging phenomena (Table 3). In the case of P-100/ $AlCl_3$ , attainment of the first stage is rapid ( $\sim 1$  day), and the fibers even acquire the blue-black color characteristic of  $AlCl_3$ -rich compounds. Intercalation with  $FeCl_3$  proceeds with considerably more difficulty -- as in other graphites -- giving mixed stages. It should be emphasized that reaction conditions other than those essayed in this study may exist at which pure stages can be formed.

Unfortunately, the environmental stability of trichlorides in these fibers is extremely poor (Figure 5).  $AlCl_3$  and  $FeCl_3$  fibers are rapidly and irreversibly hydrated (i.e., drying does not yield the original staged GIC) on exposure to ambient humidity. Both Fig. 4 and TGA results [7] suggest that intercalated P-100 fibers are the more stable.

3.3 Intercalated fiber composites

In Figure 6, preliminary mechanical and electrical property data are presented for GY-70 fiber composites and 3% residual nitrate (after desorption)

intercalated GY-70 composites. The matrix material is Epon 828 with 70 phr Versamid 140, cured at room temperature. The paucity of data reflects difficulties in lab scale composite fabrication techniques. The results indicate that significant improvement in composite electrical properties can be obtained with little, if any, compromising of mechanical integrity. It should be emphasized that the level of residual intercalant (3%) is less than half of the maximum possible (8-10%); it will be interesting to see what further gains in conductance can be achieved at higher nitrate loading. Finally, there is abundant evidence that the presence of polar functionality at the fiber-matrix interface increases susceptibility to hydrolytic degradation of composites[6]. Further studies of intercalated fiber composites must address this issue as well, as long-term stability is critical for the practical application of these materials.

#### Acknowledgment

This work was supported by the U.S. Army Research Office through Grant Number DAAG29-79-C-0208.

## REFERENCES

1. S. Flandrois, Proc. Symp. on Intercalated Graphite, Materials Research Society, in press
2. H. Selig, M. Rabinovitz, I. Agranat, C. H. Lin and L. Ebert, J. Am. Chem. Soc., 99, 953 (1977)
3. C. Herinckx, R. Perret and W. Ruland, Nature, 220, 63 (1968)
4. T. Dziemianowicz, K. Leong and W. Forsman, Proc. Symp. on Intercalated Graphite, Materials Research Society, in press
5. W. Forsman, F. Vogel, D. Carl and J. Hoffman, Carbon, 16, 269 (1978)
6. Y. Ko, W. Forsman and T. Dziemianowicz, Poly. Eng. Sci., 22, 805 (1982)
7. T. Dziemianowicz, Ph.D. Thesis, University of Pennsylvania, 1983
8. F. Vogel, Fourth London Intl. Conf. on Carbon and Graphite, 332 (1974)
9. J. Barker and R. Croft, Aust. J. Chem., 6, 302 (1953)
10. J. Hooley, W. Garby and J. Valentin, Carbon, 3, 7 (1965)
11. K. Bardhan and D. Chung, Ext. Abs. Prog., 14th Bienn. Conf. Carbon, 282 (1979)
12. W. Metz and L. Siemsgluss, Mat. Sci. Eng., 31, 119 (1977)
13. D. Nixon, G. Parry and A. Ubbelohde, Proc. Roy. Soc., 291A, 324 (1966)
14. J. Hooley, Ext. Abs. Prog., 12th Bienn. Conf. Carbon, 73 (1975)
15. P. Kwizera, M. Dresselhaus and G. Dresselhaus, Ext. Abs. Prog., 15th Bienn. Conf. Carbon, 100 (1981)
16. H. Oshima, J. Woolam, A. Khan, E. Haugland, M. Dowell and B. Brandt, Ext. Abs. Prog., 15th Bienn. Conf. Carbon, 66 (1981)
17. T. Chieu, G. Timp and M. Dresselhaus, Proc. Symp. on Intercalated Graphite, Materials Research Society, in press

TABLE 1

KINETIC PARAMETERS OBTAINED FROM NUCLEATION/PENETRATION MODEL

GRAPHITE TYPE	PARTICLE SIZE	$T_{\text{HNO}_3}$ (C) <sup>3</sup>	$\Delta M_{\infty}/M_0$	$\tau_N$ (sec)	$\tau_D$ (sec)	$\theta$ ( $\tau_D/\tau_N$ )
HOPG	5 mm	15	0.502	800	3180	3.98
Powder	44 $\mu\text{m}$	15	0.492	1040	290	0.28
GY-70	8 $\mu\text{m}$	15	0.347	4650	1030	0.22
		10	0.330	10800	980	0.09
P-100	11 $\mu\text{m}$	15	0.467	2000	605	0.30
		11	0.364	3700	605	0.16

TABLE 2  
 STAGING IN HNO<sub>3</sub> INTERCALATED FIBERS

Stage	Pristine	Stage 2	Stage 3	Stage 4
GY-70	$I_c = 3.4 \text{ \AA}$	$11.1 \text{ \AA}$	$14.5 \text{ \AA}$	
P-100	$I_c = 3.39 \text{ \AA}$		$14.6 \text{ \AA}$	$17.8 \text{ \AA}$

TABLE 3  
TRICHLORIDE INTERCALATED FIBERS

INTERCALANT	FIBER	TEMP. (C°)	TIME (D.)	$\Delta M_{\infty}/M_0$	STAGE	R/R <sub>0</sub>
AlCl <sub>3</sub>	GY-70	180/200	2	0.65	2(1)	0.13*
	P-100	180/200	1	1.28	1	
FeCl <sub>3</sub>	GY-70	290/300	4	0.70	G,1,2	0.26 <sup>+</sup>
	P-100	280/300	3	0.98	Z(G)	

Resistances measured in nitrogen (\*) or air (+)

FIGURE CAPTIONS

- Figure 1. Kinetic data and best fit to equation (1) for  $\text{HNO}_3$  intercalation of GY-70 fibers ( $T_G=22^\circ\text{C}$ ).
- Figure 2. Kinetic data and best fit to equation (1) for  $\text{HNO}_3$  intercalation of P-100 fibers ( $T_G=22^\circ\text{C}$ ).
- Figure 3. Normalized resistance change on  $\text{HNO}_3$  intercalation of HOPG and graphite fibers. Arrows indicate the weight uptake corresponding to 90% of final resistance change.
- Figure 4. Long-term environmental stability of  $\text{HNO}_3$  intercalated fibers in ambient air ( $\bullet, \blacktriangle$  freshly intercalated;  $\circ, \triangle$  desorbed;  $R_0$  refers to resistance of pristine fiber).
- Figure 5. Hydration of  $\text{AlCl}_3$  intercalated fibers in ambient air.
- Figure 6. Interlaminar shear strength (top) and resistivity<sub>f</sub> (bottom) of pristine fiber ( $\circ$ ) and 3% residual nitrate intercalated fiber ( $\bullet$ ) composites. Dotted line indicates hypothetical  $\rho-V_f$  relationship for composites containing fibers of the indicated resistivity.

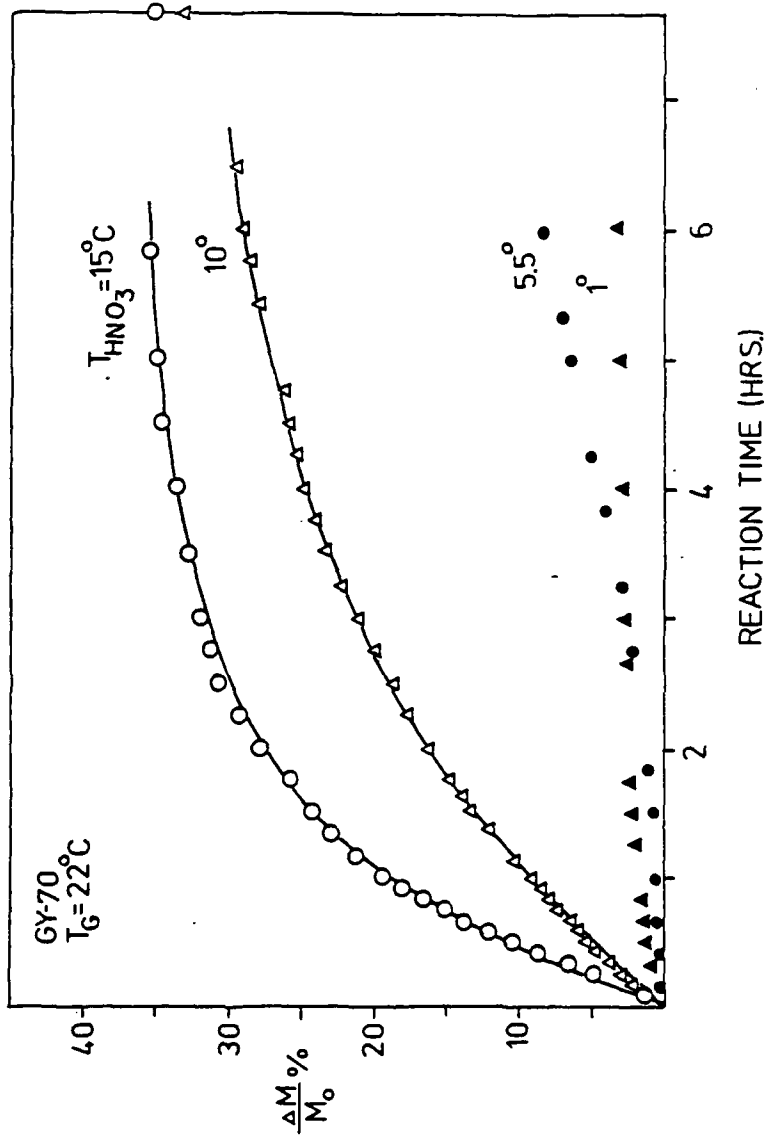
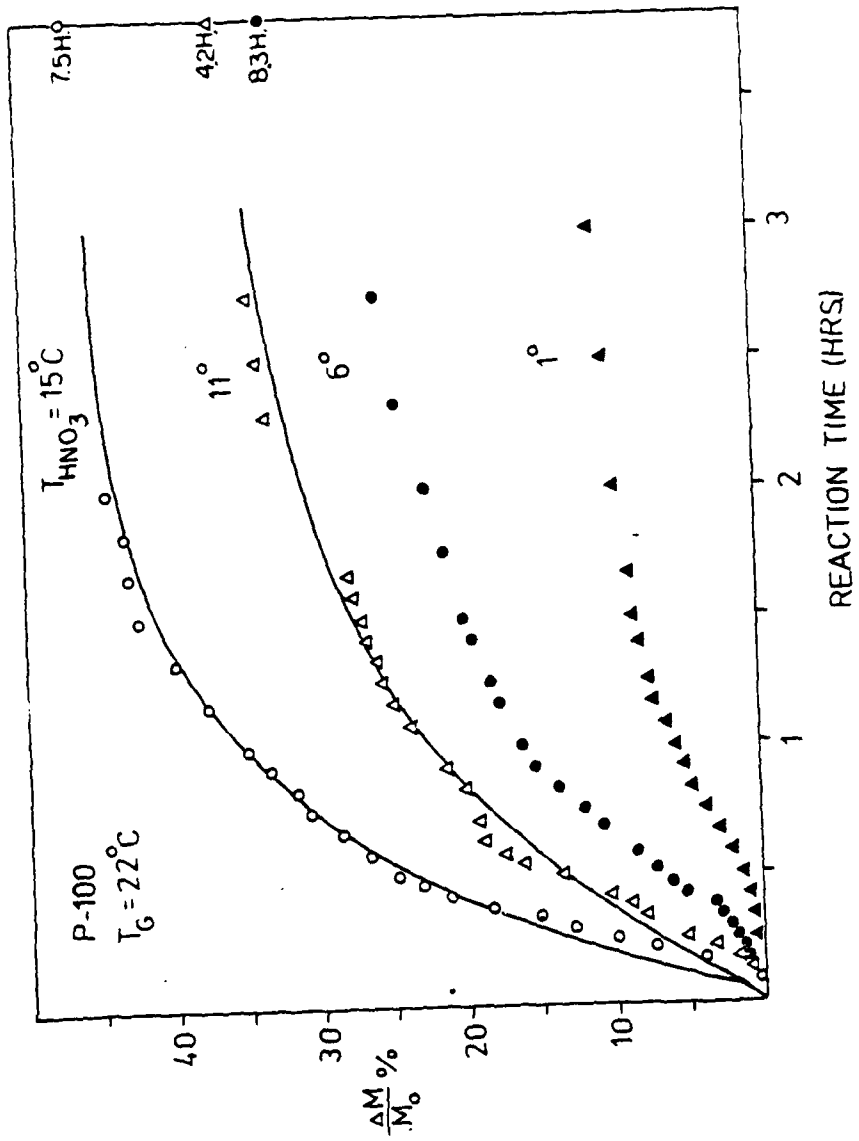
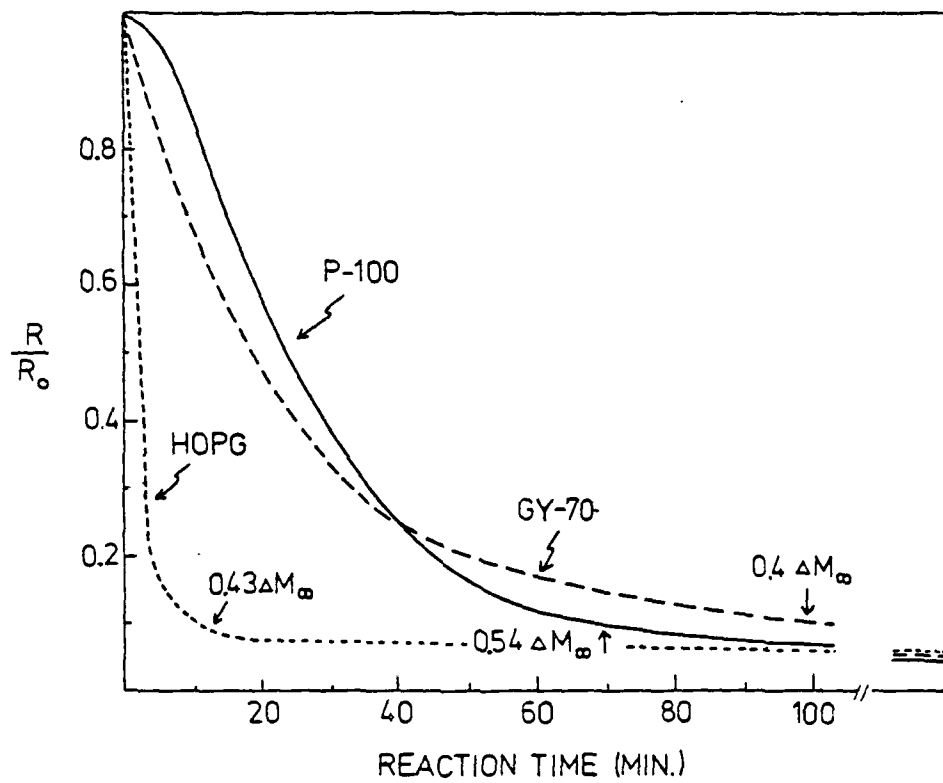
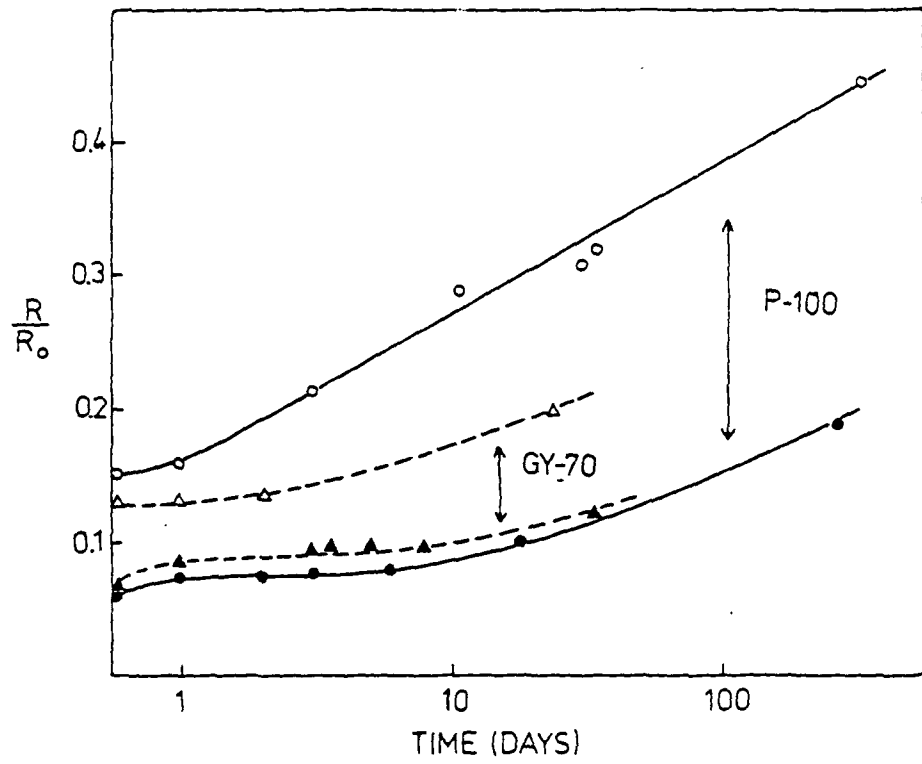
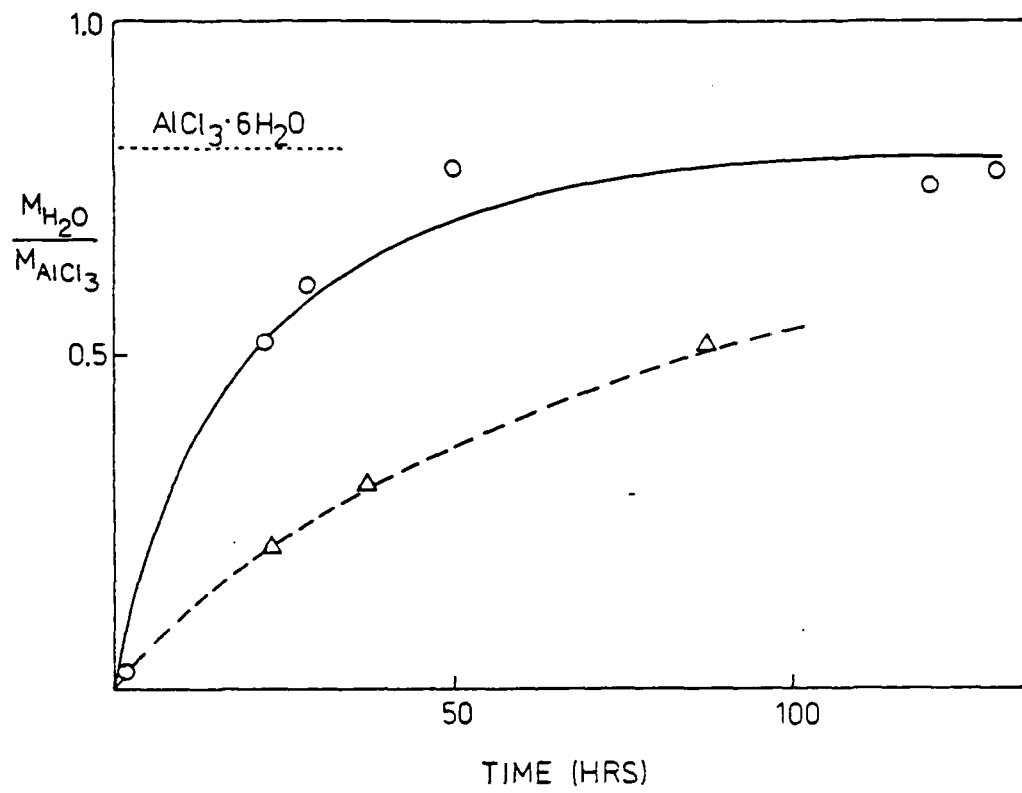


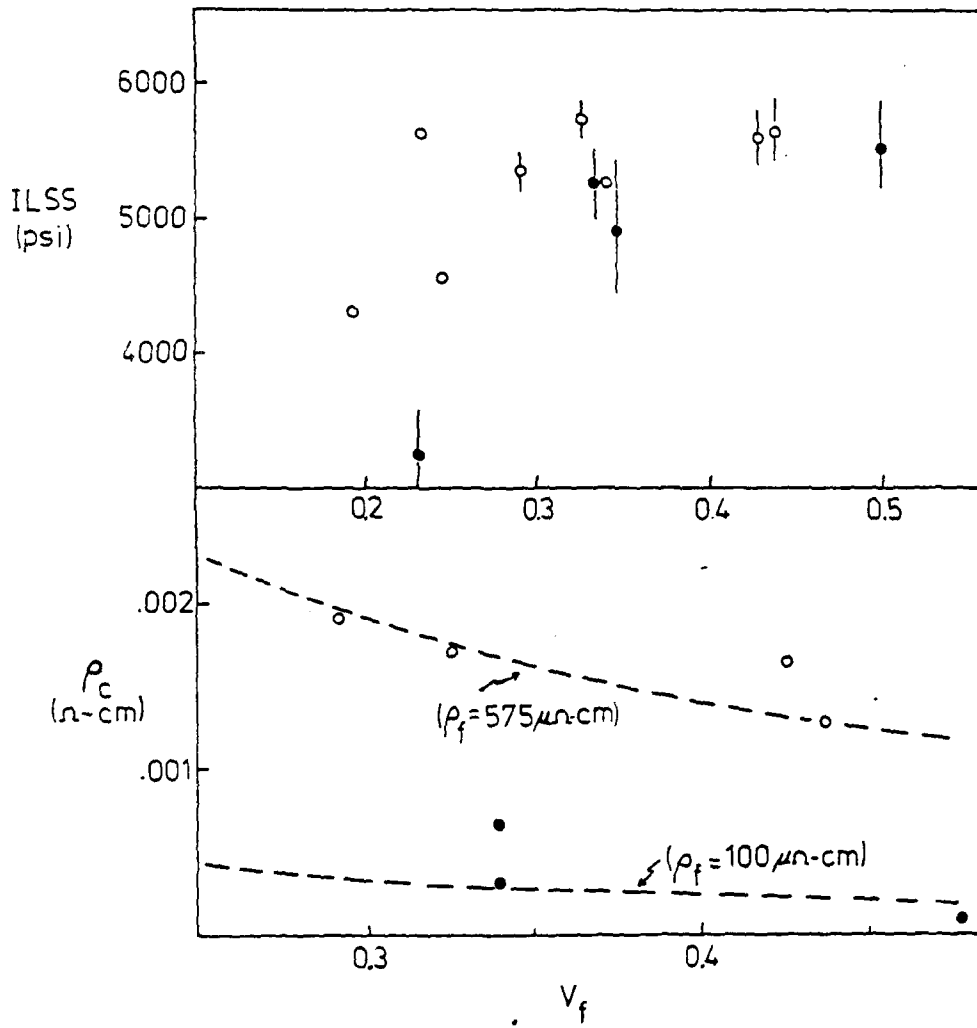
Fig. 1









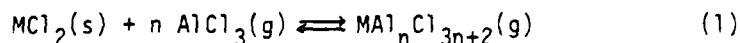


[Appendix 7]

PRELIMINARY RESULTS ON THE SYSTEM GRAPHITE-MCl<sub>2</sub>-NO

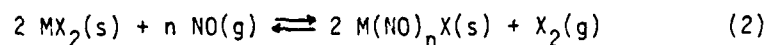
K. Leong, A. Tome, T. Dziemianowicz and W. Forsman  
Department of Chemical Engineering  
University of Pennsylvania  
Philadelphia, PA 19104

The use of complexing agents to facilitate intercalation into the graphite lattice is receiving growing attention. Stumpp's initial report [1] alerted researchers in the field to the utility of this synthetic route in the case of transition metal dichlorides. Here, a more volatile trichloride -- such as AlCl<sub>3</sub> or FeCl<sub>3</sub> -- can be used to enhance vapor phase transport of the non-volatile dichloride:

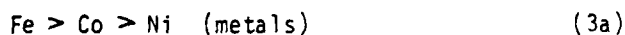


Subsequent work has shown that reduced temperatures and reaction times are not the only benefit; MnCl<sub>2</sub> compounds prepared via this route show long range order which cannot be reproduced in the direct synthesis [2,3], and NiCl<sub>2</sub> has been inserted to the first stage -- in a graphite fiber, no less -- whereas stage 2 is the richest level previously encountered [4,5]. Equally striking results have been obtained with liquid phase complexes of the alkali metals [6].

Due to its electronic structure -- six bonding and one anti-bonding valence electron -- nitric oxide (NO) is a willing electron donor, and hence forms complexes with a number of transition metals and their compounds. In particular, a number of metal nitrosyl halides are known [7]:



These are reported to be low subliming compounds with ease of formation in the order



We have attempted to intercalate dichlorides into HOPG and natural powder via metal nitrosyl halide complexes, using the conventional "tube a deux boules" technique, with graphite and intercalant in separate bulbs, and under a pressure (at 23°C) of 500 torr of NO. Results to date are as follows:

	Graphite	T(°C)	Time	Comments
FeCl <sub>2</sub>	HOPG	250		reacting slowly
		400	5 d. 33 d.	R/R <sub>0</sub> =0.49 R/R <sub>0</sub> <sup>0</sup> =0.22
	Powder	350,400	5d.	no reaction
NiCl <sub>2</sub>	HOPG	350,500	5 d.	no reaction
	Powder	350	5 d.	no reaction
		500	5 d.	Δm/m <sub>0</sub> ~ 50%; powder pattern shows G plus possible stage 4
MnCl <sub>2</sub>	HOPG	400	>10 d.	no reaction

Resistance measurements indicate that in the case of FeCl<sub>2</sub> intercalation is clearly taking place; this is a reproducible effect. Success with iron chloride always raises the question of FeCl<sub>3</sub> -- as opposed to FeCl<sub>2</sub> -- insertion. X-ray results are pending on these samples, and it is hoped that future experiments designed to eliminate this possibility will resolve this issue. It may also prove interesting to conduct studies at lower temperatures, perhaps ≤ 200°C (at which these complexes are reputedly more stable) and to look at other metal halide systems.

#### Acknowledgment

This work was supported by the U.S. Army Research Office through Grant Number DAAG29-79-C-0208.

## REFERENCES

1. E. Stumpp, Mat. Sci. Eng., 31, 53 (1977)
2. T. Dziemianowicz, R. Vangelisti, A. Herold and W. Forsman, Carbon, in press
3. F. Baron, S. Flandrois, C. Hauw, J. Gaultier, Solid State Comm., 42, 759 (1982)
4. T. Chieu, G. Timp and M. Dresselhaus, Proc. Symp. on Intercalated Graphite, Materials Research Society, in press
5. S. Flandrois, J. Masson, J. Rouillon, J. Gaultier and C. Hauw, Synth. Metals, 3, 1 (1981)
6. . Besenhard, Proc. Symp. on Intercalated Graphite, Materials Research Society, in press
7. C. Addison and J. Lewis, Quart. Rev.,   , 115 (195 )

[Appendix 3]

DSC AND TGA OF INTERCALATED GRAPHITE FIBERS: A STUDY OF  
STRUCTURE AND DEINTERCALATION

W.C. Forsman and T.S. Dziemianowicz  
Department of Chemical Engineering  
University of Pennsylvania  
Philadelphia, Pennsylvania 19104

Work from this laboratory has demonstrated that intercalated graphite fibers show promise in the fabrication of high-strength, highly electrically conducting composite materials.<sup>(1,2)</sup> Of critical importance, however, is the stability - both thermal and environmental - of the intercalated graphite fiber. This paper reports DSC and TGA studies of graphite fiber intercalated with nitric acid, along with isothermal deintercalation experiments, which give insight into the structure and stability of the intercalated fiber.

The fibers studied were Celanese GY-70 and Union Carbide P-100. The GY-70 had an average density of 1.96 g/cm<sup>3</sup>, a diameter of 8.4  $\mu$ m and an electrical resistivity of 650  $\Omega$  cm. The P-100 demonstrated somewhat higher crystalline perfection; its average density was 2.15 g/cm<sup>3</sup>, it had a diameter of 11  $\mu$ m and an electrical resistivity of 250  $\Omega$  cm. Intercalations were performed in equipment described previously<sup>(3)</sup>, which was modified to accommodate fiber specimens. The graphite fiber was kept at room temperature and the nitric acid reservoir at 15°C.

Electrical resistance of single fibers was determined before and after intercalation and while being subjected to isothermal deintercalation by the four-point method<sup>(4)</sup>. X-ray patterns were obtained by the Debye-Scherrer technique. DSC, TGA and weight loss measurements during isothermal deintercalation were done on fiber bundles.

Before discussing the results of our experiments on intercalated fiber, we should review some features of deintercalation of highly oriented pyrolytic graphite (HOPG). A stage-2 nitrate compound prepared from HOPG can be deintercalated under isothermal conditions by first reducing the vapor pressure of HNO<sub>3</sub> in equilibrium with the intercalation compound and then exposing the specimen to dynamic vacuum. In carrying out such an experiment, we found that in going from stage-2 to stage-4, there was no change in electrical conductivity.<sup>(5)</sup> If deintercalation is performed sufficiently slowly, however, there is a transformation from the  $\alpha$  form to the  $\beta$  form of the nitrate compound which occurs with loss of intercalant but without change in stage. In the transformation of a stage-2 compound the stoichiometry is reported to go from "C<sub>10</sub>HNO<sub>3</sub>" to "C<sub>16</sub>HNO<sub>3</sub>" (these empirical stoichiometries ignore the small molecular weight difference between HNO<sub>3</sub> and NO<sub>3</sub><sup>-</sup>). This transition is associated with the loss of about one third of the original intercalant. The  $\beta$  form is reported to be the more stable of the two.<sup>(6,7)</sup> Indeed the  $\beta$  form of HOPG nitrate has been reported stable to vacuum,

and in a dry atmosphere for over a year.

Graphite nitrate fiber demonstrates somewhat different deintercalation behavior. Figure 1 shows weight loss and increase in electrical resistivity of GY-70 and P-100 graphite nitrate fibers when subjected to the same deintercalation conditions described above for the HOPG compound. After reducing the partial pressure of  $\text{HNO}_3$  in equilibrium with the intercalated fiber to zero, the fibers were subjected to dynamic vacuum for up to 24 hours. X-ray results indicated a rapid transformation to the  $\alpha$  form during deintercalation of the P-100 fiber. (Although the GY-70 fiber was not x-rayed, we assume the same transformation took place.) Weight loss was continuing and resistivity still increasing after 20 hours. Figure 2 shows increasing resistivity with time for fibers as-intercalated and subjected to isothermal deintercalation under dynamic vacuum for 12 hours before exposing to a dry atmosphere. Unlike the results reported for analogous HOPG compounds the fiber nitrates continued to degrade, at least to the extent that "quality" is determined by electrical conductivity, for 200 days with no indication that the rate of degradation was decreasing.

Figure 3 shows TGA and DSC measurements of P-100 fiber intercalated to stage-4 by nitric acid. Results are given for freshly intercalated fiber, fiber that had been reduced to about 20% weight gain by exposure to dry air, and fiber which had been exposed to dynamic vacuum for 10 hours. We note that the as-intercalated specimen loses about one third of its intercalant by about 60°C with the maximum rate of loss at about 43°C. Since, according to Fuzellier, et al.<sup>(6,7)</sup>, this loss is very nearly that amount associated with an  $\alpha + \beta$  transition, we suggest that this is indeed the physical change associated with the large endothermic transition. In the case of fiber that had been exposed to air, this transition would have been largely complete before the TGA and DSC experiments were performed. There is, however, further endothermic weight loss with a maximum rate at about 70°C which we associate with further loss of neutral  $\text{HNO}_3$ . We suggest that the rate of thermal deintercalation of the as-intercalated fiber is too slow to allow the as-intercalated TGA curve to "catch up" with that of the air-deintercalated fiber.

The fiber that had been exposed to dynamic vacuum was essentially stable up to 100°C. There is, however, an intriguing transition at 80°C (probably masked in the air-deintercalated specimen). At present, we offer no suggestions as to the physical origin of this transition.

Acknowledgment This work was supported by the Army Research Office through grant DAAG29 79 C 0208.

1. T.S. Dziemianowicz and W.C. Forsman, accepted by Synthetic Metals.
2. W.C. Forsman, F.L. Vogel, C. Zeller and T.S. Dziemianowicz, submitted to Synthetic Metals.
3. W.C. Forsman, F.L. Vogel, D. Carl and J. Hoffman, Carbon, 16, 269 (1978).
4. F.L. Vogel, Fourth London Int'l. Conf. on Carbon and Graphite, 332 (1974).

5. W.C. Forsman, D. Carl and F.L. Vogel, Mat. Sci. and Eng. 47, 187 (1981).
6. H. Fuzellier, F. Rousseaux, J.-F. Mareche, E. McRae and A. Herold, Extended Abstracts, 15th Biennial Conf. on Carbon, 393 (1981).
7. R. Moret, R. Comes, G. Furdin, H. Fuzellier and F. Rousseaux, Transactions of the Annual Meeting of the Materials Res. Soc., 1982, in press.

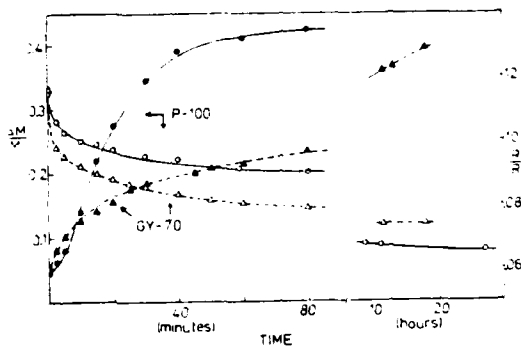


Figure 1 Weight loss and resistance change on isothermal deintercalation of P-100 and GY-70 nitrate fibers.  $M_0$  and  $R_0$  are initial mass and resistance,  $\Delta M = M - M_0$  where  $M$  is the mass of the intercalated fiber, and  $R$  is resistance.

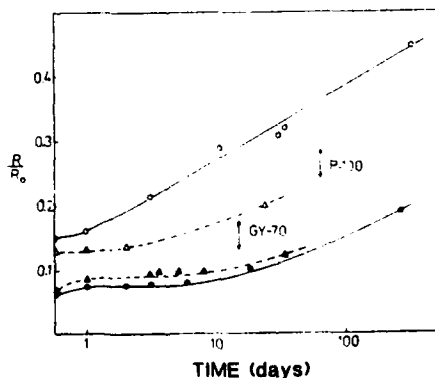


Figure 2 Stability of nitrated fibers as measured by resistance increase;  $R_0$  is resistance before intercalation. Solid symbols represent deintercalation in air, open symbols represent deintercalation in air after exposure to 10 hours of dynamic vacuum.

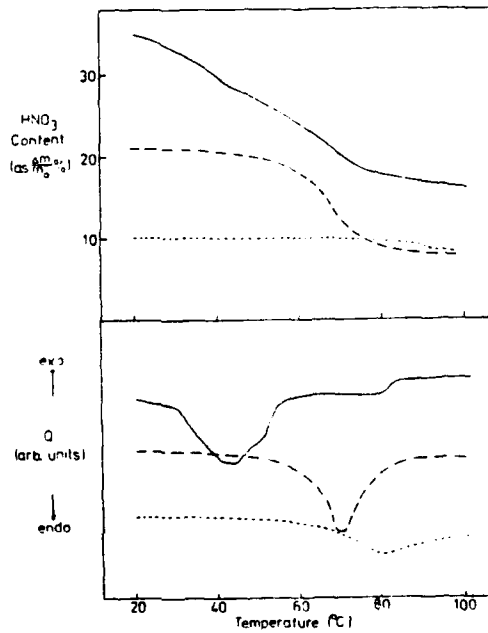


Figure 3 Thermogravimetric analysis and differential scanning calorimetry of freshly intercalated P-100 fibers (—), air-deintercalated fibers (---), and vacuum deintercalated fibers (.....).

[Appendix 9]

Letter to the Editor

of CARBON

INTERLAMINAR SHEAR-STRENGTH OF EPOXY COMPOSITES  
FABRICATED FROM INTERCALATED GRAPHITE FIBER

We recently published results of interlaminar shear strength measurements (by the short-beam shear technique) for epoxy composites fabricated from pristine GY-70 fiber (courtesy of Celanese Corporation) and GY-70 fiber that had been lightly intercalated by nitric acid.<sup>(1)</sup> Although there was no measurable degradation of interlaminar shear strength associated with intercalation, the test left something to be desired in that the fibers used in the composites had only 3% by weight residual intercalant after neutral spacers had been removed under vacuum.<sup>(2)</sup> It might be noted, however, that this residual intercalant is associated with an increase of a factor of five in electrical conductivity of the fiber and an increase of a factor of 14 in the in-plane electrical conductivity of 90° ply composites of 50 volume % fiber.<sup>(3)</sup> So it is clear that the fiber used in these experiments<sup>(1)</sup> was intercalated and not merely surface treated.

We should now like to present data on interlaminar shear strengths determined on composites prepared from more heavily intercalated fiber - namely 10% residual intercalant after removal of neutral spacers. Other than the extent of intercalation, the experiments were done as reported previously.

The results are shown in Table 1. One should note that, in these experiments, the short-beam shear strengths of the unintercalated fiber

composites were lower than those reported previously<sup>(1)</sup> - about 4000 vs 5000 psi. We should like to point out, however, that the fiber distribution was not as uniform in these specimens as they were in the specimens used previously, and we feel confident that this explains the poorer performance of the composites. What we wish to point out, however, is that, within this series of experiments on composites we suggest are comparable, the specimens fabricated from intercalated graphite fiber demonstrate about 25% improvement in interlaminar shear strength.

Table 1

Results of Short-Beam Shear Tests

Celanese GY-70 -- Epon 828 Cured with Versamide 125

Fiber Treatment	Volume Fraction Fiber*	Short Beam Shear Strength (psi)	# Samples
Series 1			
Virgin	~ 25%	4055 $\pm$ 90	4
10% HNO <sub>3</sub>	~ 25%	5080 $\pm$ 520	4
Series 2			
Virgin	~ 35%	3330 $\pm$ 500	3
10% HNO <sub>3</sub>	~ 35%	5060 $\pm$ 70	4

\*Volume fraction constant within each series, although exact value unknown.

## Acknowledgment

This work was supported by the Army Research Office through  
Grant Number DAAG 29-79-C-0208.

W. C. Forsman

T. S. Dziemianowicz

Department of Chemical Engineering  
University of Pennsylvania  
Philadelphia, Pennsylvania 19104

## References

1. T.S. Dziemianowicz and W.C. Forsman, accepted by Synthetic Metals
2. W.C. Forsman, D.E. Carl, and F.L. Vogel, Mater. Sci. Eng., 47,  
187 (1981).
3. W.C. Forsman, F.L. Vogel, and C. Zeller, submitted to Synthetic  
Metals.

[Appendix 10]

ELECTRICAL CONDUCTIVITY OF COMPOSITES  
FROM INTERCALATED GRAPHITE FIBER

W.C. Forsman\*, F.L. Vogel\*\*, C. Zeller\*\*\*

College of Engineering and Applied Science  
University of Pennsylvania  
Philadelphia, PA 19104

It is well known that intercalation of natural or highly oriented pyrolytic graphite can increase basal plane electrical conductivity by a factor of 10-15<sup>(1)</sup>, and increases as high as a factor of 20 have been reported<sup>(2)</sup>. The in-plane conductivity of even graphoil can be increased by a factor of 14.6 by intercalating with  $\text{FeCl}_3$ <sup>(3)</sup>. In the case of graphite fibers, intercalation has been reported to effect an increase in fiber-axis conductivities by as much as a factor of 50, probably because insertion of molecules and ions increase the crystalline order of the host graphite as well as changing electronic properties<sup>(4)</sup>. Since electrical conductivity of composites fabricated from graphite fibers is a property of great interest, we set out to explore the feasibility of preparing composites of intercalated graphite fiber, and to determine how increased fiber conductivity is reflected in increased conductivity of the composites. As a prototype intercalation compound, we elected to study fibers of graphite nitrate.

\* Department of Chemical Engineering  
\*\* Department of Electrical Engineering and Science  
\*\*\* Present address: Pitney-Bowes Corp.,  
Norwalk, CT 06852

Before considering the fabrication of composites, it is critical that one take note of some of the important aspects of intercalation chemistry - a subject rapidly growing in maturity<sup>(5)</sup>. If we consider so called acceptor compounds, it is of special importance to recall that the interlamellar regions of intercalation compounds can be considered to accommodate both ions and neutral molecules. In principle, it is possible to remove the neutral molecules under vacuum. In many instances, however, it is probably safe to assume that the neutral molecules would be "frozen" into an intercalation compound under conditions for which it might be used in a fiber-polymer composite - for example, the  $MnCl_2 - AlCl_3$  compounds prepared at  $500^\circ C$ <sup>(6)</sup>. On the other hand, there are two examples of graphite intercalation compounds, the  $HNO_3$  and  $AsF_5$  compounds, for which neutral (and highly corrosive) species can be moved in and out of the interlamellar regions by adjusting their partial pressure in the atmosphere in equilibrium with the compound. It seems reasonable, then, that any corrosive, labile molecular species should be removed from the interlamellar regions of the intercalation compound before attempting the fabrication of composites from intercalated fiber.

Experiments were done with Celanese GY70 fibers. Intercalation experiments were run in apparatus described previously<sup>(7)</sup>. In this case, however, graphite fiber tow was hung in the intercalation chamber along with a small sample of tow which was suspended from the quartz spring balance. Preliminary experiments demonstrated that the percentage weight uptake of the large tow (obtained by removing the sample from reactor

and weighing on an analytical balance) was essentially the same as that recorded for the small sample suspended from the quartz balance. Fiber was intercalated to second stage at room temperature (about 25°) with nitric acid prepared as described in an earlier paper<sup>(7)</sup> and supplied from a reservoir at  $20.0 \pm 0.1^\circ\text{C}$ . After removing "neutral spacers" under vacuum as described previously<sup>(8)</sup>, the intercalated fibers were ready for fabrication into composites with Stycast #1264 commercial epoxy resin.

Before compositing, intercalated fibers were kept in a dessicator with anhydrous  $\text{CaSO}_4$ . Composites were layed up by hand in a teflon mold in the laboratory, with no special provision to protect the fiber from the atmosphere. Uniaxial samples were laid up from pristine fibers as well as composites in which 10 or 11 ply of fibers were arranged 90° to each other. Only 90° ply composites were fabricated from intercalated fiber. Composites were cured at room temperature for 48 hours. The volume fraction of fiber in a composite was estimated from the weights of resin and the finished composite. This estimation introduced the most significant error in interpreting conductivity data.

It is important to note that composites fabricated from intercalated fiber from which neutral  $\text{HNO}_3$  had been removed remained unchanged in appearance for months when left on the laboratory bench. For completeness, duplicate experiments were run with fiber from which no neutral  $\text{HNO}_3$  had been removed. In each case, the composites began spontaneous delamination before complete cure of the resin could take place.

Electrical conductivity of fiber before and after intercalation was determined by the contactless technique developed at this University<sup>(9)</sup> using small loops of tow joined by gold paste. Measurement of seven tow specimens gave a fiber-axis resistivity of  $5.84 \times 10^2 \mu\Omega \text{ cm}$  with a standard deviation of  $0.20 \times 10^2 \mu\Omega \text{ cm}$ . Three samples of the intercalated tow gave an average resistivity of  $1.25 \times 10^2 \mu\Omega \text{ cm}$  with a standard deviation of  $0.12 \mu\Omega \text{ cm}$ . Resistivities of  $35 \times 35 \times 3 \text{ mm}$  specimens cut from the molded composites were also determined by the contactless technique<sup>(9)</sup>. The results are shown on a log-log plot in Figure 1.

In applying the contactless technique to uniaxial composites with fibers running parallel to the specimen surface, the measured resistivity is an average of the resistivity in the directions parallel and normal to the fiber direction. Since the resistivity normal to the fiber direction - the so called transverse resistivity - is far greater than the resistivity in the fiber direction, the experimentally determined value of resistivity,  $\rho$ , is virtually equal to the transverse value.

One might at first assume that the  $90^\circ$  ply specimens could be considered as a stack of uniaxial composites. If this were the case, however, they would demonstrate conductivity (as determined by the contactless technique) identical to that of uniaxial specimens of the same volume fraction of fiber. Figure 1 indicates that this is not the case; the  $90^\circ$  ply specimens demonstrate resistivities an order of magnitude less than their uniaxial analogues. We interpret that behavior as a manifestation of short-circuiting between the uniaxial stacks through fiber-fiber contact.

In the limit as the volume fraction of fiber,  $f$ , approaches unity the  $90^\circ$  ply composites approach hypothetical stacks of sheets with fibers lying perfectly parallel and in perfect contact in each sheet. If we assume that the fiber-fiber contact resistance becomes negligible as  $f \rightarrow 1$ , both within and between each sheet, it is easy to show that the electrical conductivity of the stack is the same in any direction parallel to the sheets. If we further assume that the transverse fiber conductivity is negligible compared to the longitudinal fiber conductivity, the resistivity of the stack in any direction parallel to the sheets becomes equal to twice the longitudinal resistivity of the fibers. These values of limiting resistivity as  $f \rightarrow 1$  are included in Figure 1 along with resistivities of  $90^\circ$  ply composites of pristene and intercalated fiber.

The limiting resistivities as  $f \rightarrow 1$  correlate well with the experimental points of  $90^\circ$  ply composites to give the usual power-law behavior of resistivity with volume-fraction<sup>(10)</sup>. Unfortunately, however, no transverse fiber resistivities have ever been determined. There is thus no data point to include for the limit as  $f \rightarrow 1$  in a log-log  $\rho$ - $f$  correlation for uniaxial composites. Clearly, there is also too much scatter in the uniaxial resistivity data to allow for a reliable extrapolation to  $f = 1$ . For lack of a better method, therefore, the uniaxial line in Figure 1 was drawn parallel to the  $90^\circ$  ply line for pristene fiber. If we then accept the value of  $\rho$  for  $f = 1$  as realistic, Figure 1 shows that the transverse resistivity of pristene fibers is almost exactly one order of magnitude greater than the longitudinal resistivity.

The most important finding in this work, however, is the remarkable increase in the in-plane conductivities of 90° ply composites with fiber intercalation. Although intercalation increased the longitudinal conductivity of the fiber by a factor of only 4.9, the resistivity of a 50% fiber volume-fraction composite was increased by a factor of 14. This additional increase in conductivity is very likely due to decrease in fiber-fiber contact resistance due to intercalation. It should be kept in mind, however, that fiber conductivities have been increased by as much as a factor of 50<sup>(4)</sup>. If conductivity of composites scales as the conductivity of the intercalated fiber, this factor of 50 would be associated with an increase in conductivity of a 50% fiber volume-fraction composite of a factor of 140. Being somewhat more conservative, however, we feel that increasing composite conductivity by a factor of 100 is a realistic goal.

#### Acknowledgment

This work was funded in part by the U.S. Air Force Materials Laboratory, Wright-Patterson AFB, Ohio 45433, through grant AFML-TR-79-4034, and in part by the U.S. Army Research Office through grant DAAG29-79-C-0208.

#### Legend for Figure 1

A log-log correlation of composite resistivity with volume fraction of graphite fiber: (1) uniaxial composites of pristine fiber, (2) 90° ply composites of pristine fiber, (3) 90° ply composites of fiber intercalated with nitric acid. Points at  $f = 1.0$  for the 90° ply composites were calculated from the measured resistivities of the pristine and intercalated fibers.



#### REFERENCES

1. See, for example: S.C. Singhal and A. Kernick, Synthetic Metals, 3 (1981) 247; M.J. Moran, J.W. Milliken, C. Zeller, R.A. Grayeski and J.E. Fischer, Synthetic Metals, 3 (1981) 269; K. Leong, W.C. Forsman and F.L. Vogel, Extended Abstracts, 15th Biennial Conference on Carbon, (1981) 398; H. Fuzellier, F. Rousseaux, J-F. Maréché, E. McRue and A. Herold, Extended Abstracts, 15th Biennial Conference on Carbon, (1981) 393.
2. E.R. Falardeau, G.M.T. Foley, C. Zeller and F.L. Vogel, J. Chem. Soc. Chem. Commun., (1977) 389; G.M.T. Foley, C. Zeller, E.R. Falardeau and F.L. Vogel, Solid State Commun., 24 (1977) 371.
3. K. Ohhashi, S. Shimotori, I. Tsuyekawa and H. Inokuchi, Synthetic Metals, 3 (1981) 289.
4. I.L. Kalnin and H.A. Goldberg, Synthetic Metals, 3 (1981) 159.
5. W.C. Forsman, T. Dziemianowicz, K. Leong and D. Carl, Synthetic Metals, in press.
6. T. Dziemianowicz, R. Vangelisti, A. Herold and W.C. Forsman, Extended Abstracts, 15th Biennial Conference on Carbon (1981) 379.
7. W.C. Forsman, F.L. Vogel, D.E. Carl and J. Hoffman, Carbon, 16 (1978) 269.
8. W.C. Forsman, D.E. Carl and F.L. Vogel, Mater. Sci. Eng., 47 (1981) 187.
9. C. Zeller, A. Denenstein and G.M.T. Foley, Rev. Sci. Inst., 50 (1979) 71.
10. Technical Report RAD-TR-78-158, July 1978, "A Fundamental Study of the Electromagnetic Properties of Advanced Composite Materials".

END

DATE  
FILMED

8-83

DTI